INNOVATIVE TOOLS FOR OFFSHORE WIND AND DC GRIDS

Innovative tools for offshore wind and DC grids

Deliverable 1.1 – Work Package 1
Report on the evaluation of DC/DC converters, submarine cables and offshore substations on losses, cost, economy and reliability

WP1 leader	UPC
Dissemination level	Public
Website	http://innodc.org/
Grant Agreement number	765585
Due delivery	Month 12: 31 August 2018
Project dates	01/09/2017 – 31/08/2021

Summary

This paper is intended as a summary of the research performed to date by Work Package 1 of the InnoDC project. A complete inventory of electrical equipment for Offshore Wind Power Plants (OWPP) is compiled with a particular focus on cabling and DC/DC converters. Following this, design possibilities for OWPP collector and transmission topologies considering High Voltage Alternating Current (HVAC), High Voltage Direct Current (HVDC) and Low Frequency Alternating Current (LFAC) are presented. Methods of calculating life cycle costs related to initial Capital Expenditure (CAPEX), Operating Expenditure (OPEX), fixed and variable losses including Expected Energy Not Served (EENS) and reliability on both a component and system level are presented in detail with a particular focus on the HVDC Outdoor Insulation reliability. Finally, options for the formulation of an optimization problem of an OWPP is presented.

Contents

Acronyms

AC	Alternating Current
ACCB	AC Circuit Breaker
AIS	Air Insulated Switch gear
AOH	Annual Outage Hours
B2B	Back to Back
CAPEX	Capital Expenditure
CB	Circuit Breaker
CCP	Common Collector Platform
CSC	Current Source Converters
DAB	Dual Active Bridge
DC	Direct Current
DCCB	DC Circuit Breaker
DCF	Discounted Fuel Expenditures
DFIG	Doubly Fed Induction Generator
DG	Distributed Generation
DOM	Discounted Operation and Maintenance
DRU	Diode Rectifier Units
DSM	Demand-Side Management
EAF	Equivalent Availability Factor
EENS	Expected Energy Not Served
EMS	Energy Management Systems
ENTSO	European Network of Transmission System Operators
ESDD	Equivalent Salt Deposit Density
F2F	Front to Front
FCL	Fault Current Limiters
FSC	Fixed Series Capacitor

GA	Genetic Algorithm
GIL	Gas Insulated Line
GIS	Gas Insulated Switch gear
GP	Geometric Programming
GPRS	General Packet Radio Service
GSU	Generator Step Up
HMI	Human Machine Interface
HTS	High Temperature Superconducting
HV	High Voltage
HVAC	High Voltage Alternating Current
HVDC	High Voltage Direct Current
HVDC-AT	High Voltage Direct Current Auto-Transformer
IED	Intelligent Electronic Devices
IGBT	Insulated Gate Bi-polar Transistor
LAN	Local Area Network
LC	Inductive Capacitive
LCC	Line Commutated Converter
LCL	Inductive Capacitive Inductive
LCOE	Levelized Cost of Energy
LFAC	Low Frequency Alternating Current
LI	Initial Investment
LP	Linear Programming
LVDC	Low Voltage Direct Current
M2DC	Modular Multilevel DC Converter
MFT	Medium-Frequency Transformer
MI	Mineral Insulated
MINLP	Mixed Integer Non-Linear Programming
MIP	Mixed Integer Programming
MIQP	Mixed Integer Quadratic Programming

MMC	Modular Multi-Level Converter
MP	Minimal Paths
MTTR	Mean Time To Repair
MTU	Master Terminal Unit
MV	Medium Voltage
MVAC	Medium Voltage Alternating Current
MVDC	Medium Voltage Direct Current
NP	Nondeterministic Polynomial time
NPV	Net Present Value
NSDD	Non-Soluble Deposit Density
OHL	Overhead Line
OM	Operation and Maintenance
OPEX	Operating Expenditure
OSS	Offshore Substation
OWPP	Offshore Wind Power Plants
PCC	Point of Common Coupling
PE	Polyethylene
PF	Power Factor
PMSG	Permanent Magnet Synchronous Generator
PMU	Phasor Measurements Unit
PWM	Pulse Width Modulation
RBD	Reliability Block Diagram
RFC	Rotary Frequency Converter
RTU	Remote Terminal Unit
SAB	single Active Bridge
SCADA	Supervisory, Control and Data Acquisition
SDD	Salt Deposit Density
SES	Site Equivalent Salinity
SF_6	Sulfur hexafluoride

SSFC	Solid State Frequency converter
STAR	Slim Tripod Adapted for Rigs
STATCOM	Static Synchronous Compensator
SVC	Static Var Compensator
TCSC	Thyristor Controlled Series Compensation
TEP	Transmission Expansion Planning
TLP	Tension-Leg Platform
TSO	Transmission System Operators
UPS	Uninterruptable Power Supplies
VSC	Voltage Source Converter
WRIG	Wound Rotor Induction Generator
WTGT	Wind Turbine Generator Transformers
XLPE	Cross Linked Polyethylene

1 Equipment Inventory

1.1 Wind Turbines

Wind turbines convert wind energy into electrical energy. The main structural components of an offshore wind turbine are the substructure, the tower, the nacelle and the blades. Types A through D of wind turbines are classified via the electrical system housed within the nacelle [1]. Offshore wind turbines have been trending towards larger and larger units. In 2012 76% of all new offshore wind turbine models had rated capacities of 5 MW or more [2].

1.1.1 Type A: Constant Speed

Constant speed turbines as the name suggests rotate at a constant speed dictated by the grid frequency, gear box and number of pole-pairs within the generator [1]. Induction generators are used in Type A turbines as they are inexpensive and the slip adds compliance within the system [3]. Constant speed turbines are inexpensive and robust but lack the ability to extract maximum power across varying wind speeds. They also fail to provide voltage or frequency support to the grid or fault ride through capability [1].

1.1.2 Type B: Partial Variable Speed

Partial variable speed turbines attempt to improve the power extraction ability over varying wind speeds through the utilization of a converter controlled Wound Rotor Induction Generator (WRIG). By controlling the rotor resistance speeds above synchronous can be achieved allowing for better power extraction under varying wind speeds. However, the speed range is limited as excessive power dissipation in the external resistor is inefficient [1].

1.1.3 Type C: Variable Speed with partial Converter

To further improve power extraction over varying wind speeds Type C wind turbines utilize a Doubly Fed Induction Generator (DFIG). So named as the stator is connected to the grid via a step-up transformer and the rotor via a fractionally sized Alternating Current (AC) to AC converter. This set up allows for larger speed variations of -40% to 30% synchronous speed [1]. As only 20-30% of power passes through the converter, converter cost and losses are low [4]. Some grid support can be provided, however, full fault ride through capability is difficult as the stator is directly coupled to the grid. Like type B a further downside to type C turbines is the use of slip rings [5]. In the future this may be eliminated by the use of brush-less DFIG [6].

1.1.4 Type D: Variable Speed with full Converter

A type D turbine can be designed with an induction or synchronous generator. The defining characteristic is the full sized converter linking the stator to the grid. This decouples the generator allowing for fully variable speed control as well as fault ride through capability. Voltage and frequency support are possible. The main drawback of the system is the high price of the full power converter [1].

1.2 Submarine Cables

Submarine cables are used in OWPP within the Medium Voltage Alternating Current (MVAC) Collection Circuit, and for transmission from the Offshore Substation (OSS) to the Point of Common Coupling (PCC). Both three core and single core cables are available. Three core cables have the advantages of reduced losses due to magnetic field cancellation, lower installation costs and an integrated fiber optic communication cable [1]. For very high power applications, however, single core cables are utilized as they dissipate heat better. Single core cables also have the advantage of being easier to splice and in case of damage to a single conductor, the single conductor can be replaced rather than the entire cable in the case of three core cables.

1.2.1 Extruded Cables

Cross Linked Polyethylene (XLPE) Cables

In AC applications XLPE cables are utilized in both collection (MVAC) and transmission (HVAC). The insulation is extruded Polyethylene (PE) doped with chemical additives that through the process of vulcanization creates a cross linked lattice structure within the PE [7]. Cross linking imparts superior thermal properties compared to standards PE cables [8]. XLPE cables can be used on HVAC systems up to 550 kV [9]. The largest diameter cable (2500 mm^2) has an ampacity of 2.6 kA [7]. Rated voltages and diameters available are summarized in Table 1.

Table 1: Voltage rating and cross section of available AC XLPE cables [7]

Rated Voltage (kV)	Cross-section (mm^2)
66	240-2000
110	400-2500
132	400-2500
150	400-2500
220	630-2500
275	630-2500
345	800-2500
400	800-2500
500	1600-2500

XLPE cable is highly reliable and will likely last the entire lifetime of the project without problem. The most common failures (53%) offshore are caused by fishing gear and ship anchors [10]. The failure rate is 0.0307/100 km·year and the mean time to repair is 120 hours [9]. Initial capital expenditures for materials and labor (CAPEX) are high. The approximate cost per 100 km installed is 3675-4062 k€/km. Approximately 29% of the cost is for installation [9]. This average cost is deceiving, however, as AC cables are used mostly within the collection circuit. Here the cable runs are short, often less than 1 km, but still require 2 terminations and lifting into place making the installation cost a higher percentage of the CAPEX [7]. OPEX are approximately 7.3-8.1 k€/km [9].

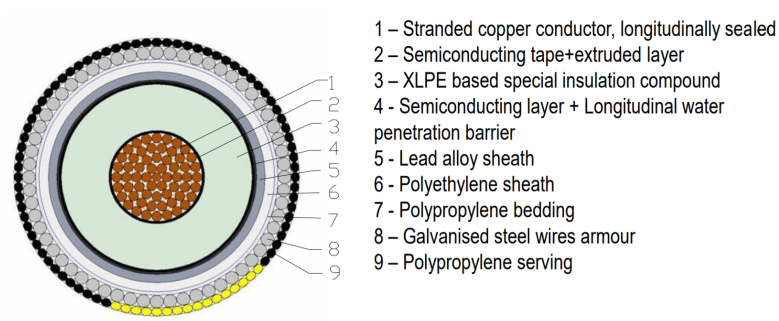

Figure 1: Layers of an XLPE HVDC cable [11]

In HVDC applications XLPE cable (Fig. 1) is only utilized with non-polarity reversing Voltage Source Converter (VSC) as polarity reversal destroys the insulation [12]. With this consideration XLPE cable has some important advantages in HVDC. The cable is easy to join, has a high temperature rating and is lighter due to the type of moisture barrier that can be used [12].

Polyethelene PE

Non cross linked polyethelene insulation is also available, however, the temperature characteristics are worse than XLPE [8]. PE cable comes in 3 densities: low, medium and high. Low density is the most flexible and high the least [13].

Ethylene Propylene Rubber (EPR)

EPR is another type of extruded cable. It is best suited for medium voltage applications as the dielectric loss factor (tanδ) and dielectric constant (ϵ_r) are both higher for EPR compared to XLPE [13].

1.2.2 Paper Mass Insulated HVDC Cables

Paper Mass Insulated HVDC Cables also called (Mineral Insulated (MI)) cables were until recently the most commonly used HVDC submarine cables. Since 2011 extruded submarine cables have seen higher utilization [7]. As dielectric loss is of no concern in Direct Current (DC) cables a high density paper of 1.0 kg/dm^3 provides the cable with both mechanical strength and high dielectric strength [13]. The cables are therefore well suited to HV applications, up to $\pm$500 kV, over long distances [9]. The cables are also suitable for deep water applications [7]. The largest diameter MI cable available is 2500 mm^2 with an ampacity of 1563 kA [9].

1.2.3 Fluid Filled Cables

Paper Insulated Oil Filled Cables

Paper Insulated Oil Filled cables have oil and paper as insulation. A low density, high permeability paper is used to minimize dielectric losses while allowing the flow of oil [13]. Paper wraps of 50 to 180 μm thickness make up the insulation. Further from the conductor the electric stress is lower and thicker wraps with lower dielectric strength can be used. The many layers of paper also provide mechanical strength [13].

High Temperature Superconducting (HTS) Cables

HTS cables are used by utilities to transmit large amounts of power over relatively short distances (<5 km) [9]. Some advantages of HTS is low losses even at lower voltage levels, environmentally benign liquid nitrogen coolant, high power density 2 to 8 times to traditional methods [14] and can be installed in existing conduit. Main disadvantages are the need for a cryogenic system and a maximum length without requiring joints of 600 m [7]. The maximum available voltage is 22 kV and ampacity 4 kA [9]

Gas Insulated Line (GIL)

No GIL systems exist offshore and few have been built on land, however, the experience of the oil and gas industry laying submarine pipe likely means it could be adapted if needed. A GIL conductor consists of a pipe filled with SF6 gas and central conductor [15].

1.3 DC/DC Converters

There are two kinds of DC/DC converters used in OWPP with DC collection systems:

1. The DC/DC converter integrated in the wind turbine. This kind of converter is used to step up the voltage from Low Voltage Direct Current (LVDC) (1-2 kV) to Medium Voltage Direct Current (MVDC) (25-40 kV). The power rating of this converter is related to the power rating of the wind turbine. High step up ratio (> 5) is required and small footprint is also important due to the cost of constructing an offshore wind turbine. Furthermore, high reliability is another feature for this converter considering the offshore environment and high maintenance cost. If a Permanent Magnet Synchronous Generator (PMSG) is used in the wind turbine, a unidirectional DC/DC converter can be considered to reduce the amount of power electronic devices and losses. If an induction generator is used, bidirectional DC/DC converters should be used because the power from grid side is required for the excitation of the induction generator [16].

2. The DC/DC converter for the offshore DC substation. This kind of converter is used to collect all the wind power from turbines and step up the voltage from MVDC (25-40 kV) to HVDC (>100 kV) to transmit the collected wind power to the onshore substation through HVDC cables. The power rating of this converter is related to the power rating of the offshore wind farm. Medium or high step up ratio (>2) is required for this converter. Small footprint is also desired to reduce the construction cost of an offshore substation. Galvanic isolation and high reliability is also essential for an offshore DC substation.

1.3.1 Classification of DC/DC converters

Before the application for Medium Voltage (MV)/High Voltage (HV) offshore DC grids, there was already many DC/DC converters proposed for other applications such as laptop power supplies, EV charger, data center, Uninterruptable Power Supplies (UPS), etc [17]. The basic requirement for DC/DC converters is the voltage stepping function. One of the simplest solutions of DC voltage stepping could be buck/boost converters as shown in Fig. 2. However the discontinuous power flow of the buck/boost converter makes it unsuitable for DC grids. Besides the buck/boost converter, there are many other two-level DC/DC converters proposed. Some of them are shown in Fig. 3 [18, 19, 20]. Fig. 3a is the Dual Active Bridge (DAB). The bidirectional power flow of DAB can be easily controled using phase-shifting modulation. The Medium-Frequency Transformer (MFT) is used in DAB to increase the power density. For some applications which need unidirectional power flow, a single Active Bridge (SAB) as shown in Fig. 3b can be adopted instead of DAB to reduce the number of Insulated Gate Bi-polar Transistors (IGBTs) and losses. Soft switching operation can be achieved if a resonant topology in Fig. 3c is used, which can reduce the switching losses of the converter so that a higher switching frequency can be achieved to reduce the size [21]. However, all the DC/DC converters in Fig. 2 and Fig. 3 are not suitable for HVDC and MVDC grids due to high power ratings and high dv/dt stresses. A series connection of IGBTs is required to withstand high voltage, so the dynamic voltage sharing on the IGBTs is another issue for these converters if they are used for DC grids [22].
As is mentioned above, the conventional low-power low-voltage DC/DC converters can not be used for DC grids directly. To distinguish the DC/DC converters for DC grids with the conventional DC/DC converters, the DC/DC

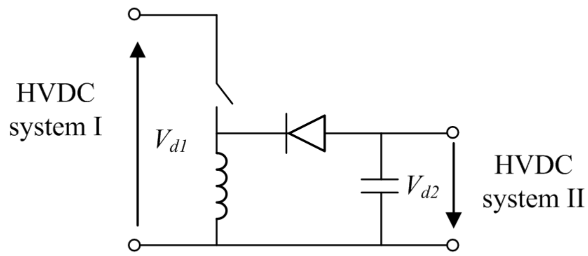

Figure 2: Buck/Boost Converter

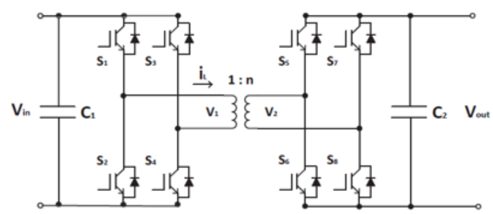

(a) Dual active bridge [18]

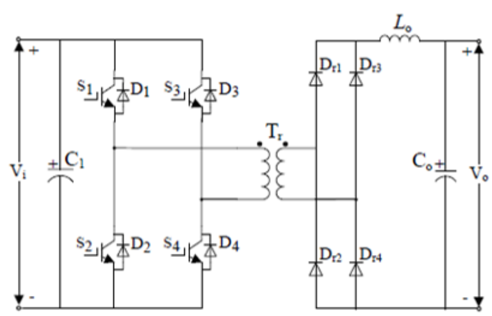

(b) Single active bridge [19]

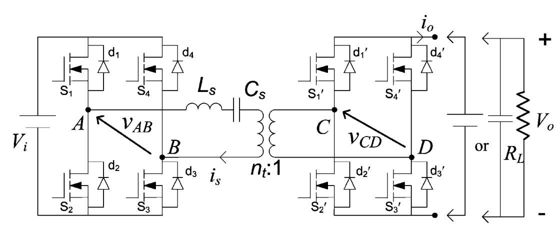

(c) Resonant dual active bridge [20]

Figure 3: Topologies of several two-level DC/DC converters

converters for DC grids are also called DC transformers, just like the AC transformers in AC grids. The features of DC/DC converters for DC grids are summarized as follows:

1. For high power and medium power applications in DC grids, DC/DC converters should be redesigned to achieve continuous power flow between two DC circuits.

2. DC/DC converters for DC grids should be able to connect two HVDC systems with the characteristics of voltage stepping, power regulation and fault isolation.

According to these features, some DC/DC converters for DC grids are proposed in the literature, which can be categorized as shown in Fig. 4. A summary of converter qualities is presented in Table 2.

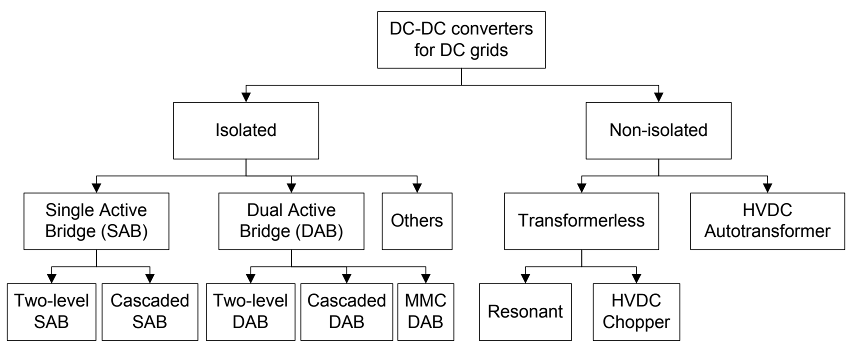

Figure 4: Topologies of DC/DC converters

1.3.2 Isolated DC/DC converters

Galvanic isolation may be needed mainly for safety and grounding reasons [23]. For example, the isolation is needed when two HVDC transmission lines with different grounding schemes are interconnected. And in some high voltage ratio applications, isolation may be needed to protect the grid on the low-voltage side from the disturbance on the high-voltage side. Isolated DC/DC converters are mainly based on the process of DC/AC/DC conversion with two DC/AC conversion stages interconnected by AC transformers or coupled inductors to realize galvanic isolation and voltage stepping.

Table 2: Characteristics of DC/DC converters for DC grids

	Galvanic isolation	Bidirectional	Fault Blocking Capability	Step ratio	Main drawbacks
Cascaded SAB	Yes	No	Yes	High	Unidirection; High insulation requirement for transformers
Cascaded DAB	Yes	Yes	Yes	High	High insulation requirement for transformers
MMC-DAB	Yes	Yes	Yes	Medium	Double conversion installed power
Resonant DC/DC converter	No	Yes	Yes	High	Design of resonant tanks
HVDC Chopper	No	Yes	Yes, requires FB SMs	High	Requires series IGBTs
HVDC-AT	No	Yes	Yes, requires FB SMs	Low	Design of AC transformer

Cascaded Single/Dual Active Bridge

One method to achieve high power and high voltage ratings is to cascade low-power low-voltage converters [24]. An input-series output-parallel (ISOP) configuration of cascaded DAB/SAB is shown in Fig. 5 [25]. The elementary converter cells can be either DAB or SAB, according to bidirectional or unidirectional power flow. On the HV terminal, the converter cells are connected in series to share the voltage while a series connection is used on the LV terminal to share the current. A high voltage ratio can be realized. Each cell only handles a fraction of the total power, thus a high switching frequency (>1 kHz) can be achieved to reduce the size and weight of AC transformers and passive components. However, the drawback of the cascaded DAB/SAB is that the insulation of the high-frequency AC transformer used in each cell should withstand the total DC voltage on the HV terminal [26]. This disadvantage limits its application to the medium voltage range.

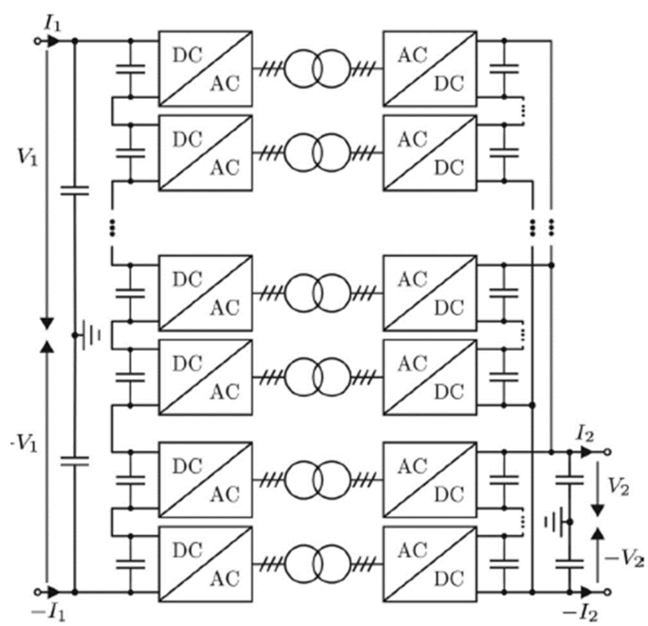

Figure 5: Cascaded DAB/SAB [25].

Modular Multi-Level Converter (MMC) DAB

A MMC-DAB is shown in Fig. 6 [27, 28]. It is also called a Front to Front (F2F) MMC and is a dual structure of the Back to Back (B2B) MMC widely used in HVDC point-to-point transmission [29]. Different modulation schemes can be used to generate different AC waveforms for the AC link such as sinusoidal, triangle and trapezoidal waveforms. Among this, the quasi-two-level modulation which generate trapezoidal AC waveforms seems to be the optimal solution considering the switching losses and overall footprint [30, 31]. The MMC-DAB can be configured either in single phase or three phases and the submodule of the MMC-DAB can be half bridge, full bridge or even direct switches [32]. Some hybrid MMC-DABs are presented in Fig. 7 [33].

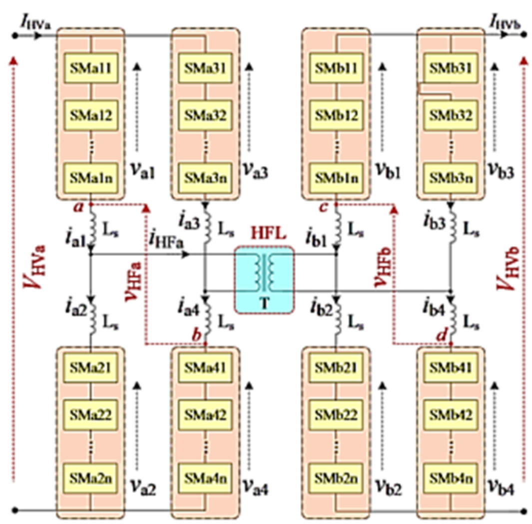

Figure 6: MMC-DAB [27]

Other isolated DC/DC converters

DAB or SAB can be recognized as transformer-based isolated DC/DC converters because AC transformers are applied to realize isolation and voltage stepping. There are some isolated DC/DC converter topologies applying coupled inductors instead of AC transformers to realize isolation. Similar to DAB/SAB, this kind of DC/DC converter can achieve high voltage and high

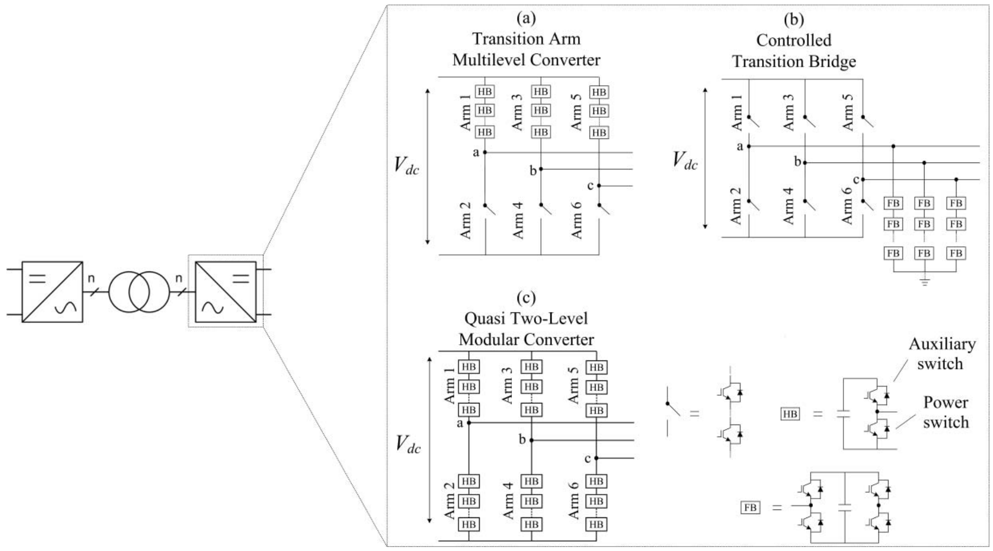

Figure 7: Hybrid MMC-DABs [33]

power ratings by cascaded connection of low-voltage low-power cell or by MMC solutions. Fig. 8 presents a cascaded DC/DC converter which applies coupled inductors for isolation [34]. Multiple coupled inductors are applied in this structure. A MMC based flyback DC/DC converter is presented in Fig. 9 which requires a centralized inductor circuit [35].
These coupled inductor based topologies are proposed for high step-up voltage ratios. However, the high insulation requirements of the coupled inductors in the cascaded structure, and the high current requirements in the centralized inductor circuits are challenging, potentially limiting these topologies to low power applications [23].

1.3.3 Non-isolated DC/DC converter

Resonant DC/DC converter

Several resonant DC/DC converters are proposed in the literature. These converters use resonant tanks (Inductive Capacitive (LC) tanks or Inductive Capacitive Inductive (LCL) tanks) to step up the voltage. The soft switching of the semiconductors can be achieved by the resonant circuits. Fig. 10 shows two LCL resonant DC/DC converters based on thyristors and IGBTs respectively [36, 37]. The power losses are minimized due to soft-switching

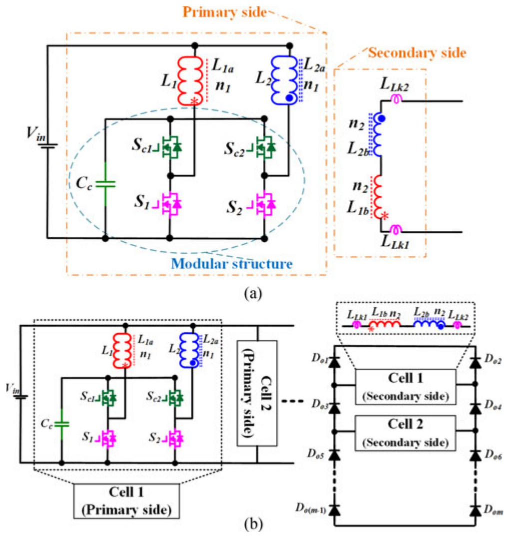

Figure 8: Cascaded DC/DC converters based on coupled inductors. (a) Basic cell structure. (b) Cascaded topology [34].

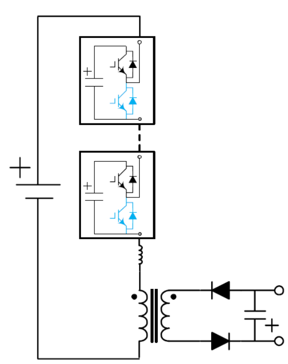

Figure 9: MMC flyback converter [35]

operation. Bidirectional power flow and a high voltage stepping ratio can be achieved. However, these resonant converters typically experience high stresses on the switches and passive components. Their lack of full modularity is also another drawback.

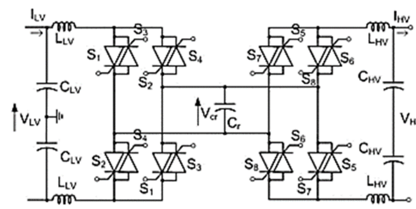

(a) Thyristor based LCL DC/DC converter [36]

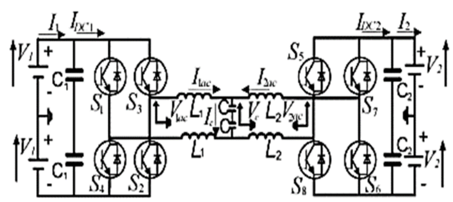

(b) IGBT based LCL DC/DC converter [37]

Figure 10: LCL resonant DC/DC converter

HVDC Chopper

Some DC/DC converters proposed for HVDC are based on conventional chopper circuits. Fig. 11 presents a HVDC-MMC chopper which replaces the semiconductors in the conventional chopper circuit with MMC submodules to achieve high power and voltage ratings. A hybrid-cascaded DC/DC converter is proposed in [38] for HVDC grids. And some derived topologies are also proposed in [38]. These hybrid-cascaded DC/DC converters have attractive capital costs, footprint, and power losses.

High Voltage Direct Current Auto-Transformer (HVDC-AT)

An HVDC-AT is shown in Fig. 13 [40, 41] which applies two MMC DC/AC converters interconnected with an AC autotransformer. The advantage of

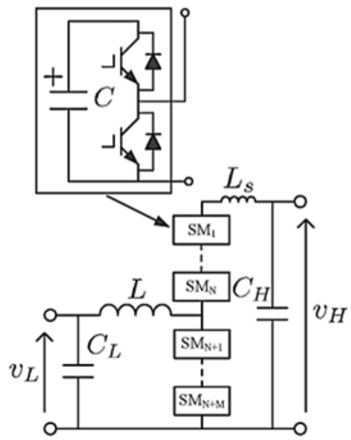

Figure 11: HVDC-MMC Chopper [39]

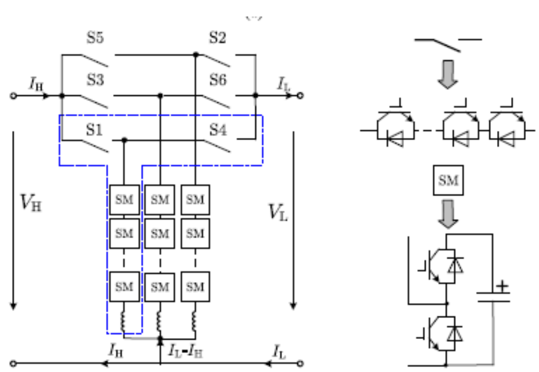

Figure 12: Hybrid-Cascaded DC/DC converter [38]

HVDC-AT is that only part of the total DC power is converted into ac power and transferred by the AC transformer. Comparing to MMC-DAB which converted the whole DC power into ac power, the HVDC-AT features higher overall efficiency and utilization of semiconductors, especially when the voltage stepping ratio is low. The problem of HVDC-AT is that both windings of the ac transformer are exposed to high DC voltage stresses, which makes it a challenge to design the ac transformer [42]. A multiport DC au-

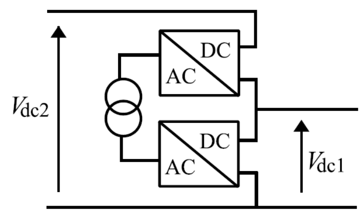

Figure 13: HVDC-AT [23]

totransformer [43] can be used to interconnect multiple HVDC systems with different voltage levels. This DC autotransformer is able to reduce 50-80% of the converter cost compared with conventional DC/AC/DC technology. Different from the conventional DC/AC/DC technology which uses magnetic coupling at the AC sides of the converters, there is direct electrical connection between the interconnected DC systems. It can achieve bidirectional power flow and fault isolation.

1.4 AC/DC Converters

HVDC technology has been proved to be more suitable than HVAC for long distance transmission [44]. There are approximately 30 HVDC point-to-point links planned or under construction in Europe in the next five years, including submarine cables and overhead lines [45]. Also, building a DC grid interconnecting HVDC links is possible. Besides, the number of offshore wind farms is increasing in Europe during recent years. Since the distance from offshore wind farms to onshore substations is also increasing, HVDC technology is used for offshore wind power transmission. The collection systems of offshore wind farms are still AC systems however. Until DC Collection grids become a reality an AC/DC converter is needed between the collection and transmission circuits.

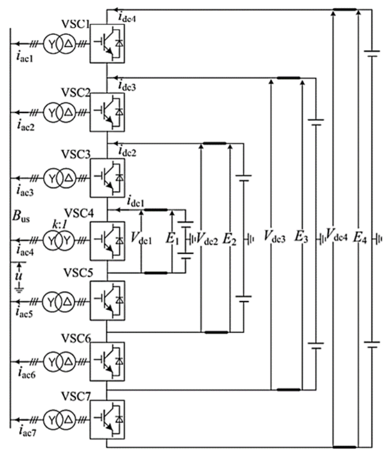

Figure 14: Multi-port DC autotransformer [43]

1.4.1 Line Commutated Converter (LCC)

Line Commutated Converter (LCC) or Current Source Converters (CSC) is a mature thyristor based technology used since the early 1950s. It is used for AC to DC conversion. Generally, LCC is used for point to point bulk power transmission although two multi -terminal connections exist. One connecting Quebec and New England in North America and the other connecting mainland Italy with the islands of Corsica and Sardinia [46], [47]. Complicated meshed multi-terminal grids may not be possible, however. In all cases the AC side grid must be robust [7] to allow LCC converters to operate in a safe manner.

LCC converters can be used for transmission distances up to 2000 km with losses of only 0.7-1.1% per station. Currently the maximum transmission capacity is 8 GW at ±800 kV converter line to ground and 5 kA. ±1100 kV is expected by 2020 [9].

A converter station is often composed of a converter, a transformer(s), reactive power compensators, harmonic filters, switchgear and auxiliary equipment, elements that are making them large and expensive [7]. A 1 GW station occupies 50000 m^2 of land and might cost approximately 110 M€. Around 37% of CAPEX is in installation. Converter lifetime is 40 years, OPEX 2% of investment per year and availability 99% [9].

1.4.2 Voltage Source Converters (VSC)

VSC is an IGBT based technology available since 1999. It is used for AC to DC conversion [7]. The MMC is the most common topology utilized for VSC transmission [1]. VSC is a self-commutated converter with better flexibility and controllability compared to LCC [7]. VSC can control both active and reactive power independently, allowing for grid support, eliminating the requirement of a robust AC side network to operate [48]. These qualities make it better suited for multi-terminal grid applications. A further benefit of VSC technology is the ability to start an entire network, i.e. black start [7].

VSC converters can be used for transmission distances up to 700 km with losses of 0.9-1.3% per station. The maximum transmission capacity is 2 GW at ±500 kV converter line to ground and 2 kA. Increases to ±800 kV, 3 kA and distances of 2000 km are expected by 2020. It has also been suggested that currently available converter capacity may be increased as much as 1.13 pu through the use of a control loop that dynamically sets current limits based on measured IGBT temperature [49].

A VSC converter station requires the same components as an LCC station, however, the converter itself is smaller and filtering requirements are lower allowing for more compact design [1, 7]. A 1 GW station occupies 18000 m^2 of land [9]. A multi level 0.9 GW offshore VSC substation occupies 50000 m^3 and has an approximate footprint of 800 m^2 [7, 50]. CAPEX, OPEX and reliability are all comparable to LCC, in the offshore case, however, the platform is considered separately [9].

1.4.3 Diode Rectifier Units (DRU)

A Diode Rectifier Units (DRU) is a new HVDC option developed specifically for OWPP transmission by Siemens and introduced in 2016. It is currently only approved for the German market [51]. The technology was originally proposed at the University of Valencia, Spain [52]. The system involves 3 pairs of DRUs connected in series producing ±320 kV for transmission. The DRU pairs are distributed across 3 small platforms. A 1.2 GW system has a combined volume of 6500 m^3 and weighs 9000 tonnes [52]. According to Siemens this is an 80% reduction in topside volume and a 65% reduction in weight compared to a 0.9 GW offshore VSC station [53, 54].

The concept has further benefits; diode technology is proven, simple and robust. The units are fully encapsulated in biodegradable material and have low losses and maintenance costs [7]. Installation can be done quicker and with fewer specialty vessels [54]. The disadvantages include the need for an auxiliary AC power supply as bi-directional power flow is not possible and a more complicated wind turbine control system to properly maintain voltage and frequency [52].

1.5 AC/AC Converters

1.5.1 AC Transformer

AC power transformers are broadly classified into transmission and distribution applications. They can then be further divided by specific application, i.e. Generator Step Up (GSU), step down, phase shifting, HVDC transformer or system intertia transformer [7]. Within the scope of OWPP, transmission transformers are of the most interest although distribution transformers may be required for some auxiliary loads.

Wind Turbine Generator Transformers (WTGT) increase the generator output to MVAC for the collector circuit. Typical voltage ratings are 10 to 36 kV [1]. Until the recent development of fire-retardant silicone or biodegradable ester liquid filled transformers, dry type were most commonly used. The cost of WTGTs is about 3% of the overall wind turbine installation [55]. On the OSS a further step up MVAC to HVAC transformer may be found in preparation for transmission to shore. Typical voltage ratings of these transformers are 36 kV to 132, 275 or 400 kV [13]. Finally, onshore a transformer will step up or down the voltage for grid connection. A phase shift or grid intertie transformer equipped with an on load tap changer may be used to provide voltage control services and facilitate the exchange of both active and reactive power [1].

Power transformers are limited in size due to transport capabilities and transport cable size rather than maximum voltage and current ratings [7]. Typical maximum ratings are 1630 MVA, 750 kV and 10 kA [9]. However, larger transformers have been built such as ABB's 1.1 kV, 10000 MW transformer for China Changji-Guquan HVDC transmission link [56, 57]. The footprint of a 765 kV transformer is 1000 m^2 [9]. In the case of a LFAC system, this footprint would increase substantially. As a rule of thumb the magnetic core size is inversely proportional to the frequency of operation. A 20 Hz transformer core would therefore be approximately 3 times the size of its 60 Hz equivalent. This is a significant barrier to the implementation of a LFAC offshore network [58].

1.5.2 Frequency Converters

Two general classes of frequency converter are available, Rotary Frequency Converter (RFC) and Solid State Frequency converter (SSFC) [59]. RFCs are a motor-generator pair with a common shaft. Multiple topologies characterized by drive motor exist [59]. Output controllability varies from the very basic up to independent frequency, voltage, active and reactive power control [60]. RFCs have a high power quality, introduce momentum into the system and provide filtering and galvanic isolation [60]. They also have both a higher mass-power and volume-power density than SSFCs. Unfortunately, RFC are limited to the voltage levels of available motor generators, about 15 kV. They also have lower efficiency, lower reliability and higher maintenance requirements compared to SSFCs [59].
Two kinds of SSFC are available. A thyristor based cycloconverter and an IGBT based VSC [61]. Cycloconverters are the less expensive option. A comparison done by Siemens for mining applications estimates a VSC costs 140% an equivalently sized cycloconverter [62]. A cycloconverter's main drawback is the need for extensive harmonic filtering and reactive compensation to satisfy grid power quality requirements [61]. The footprint of the two solutions compared by Siemens are 733 m^2 and 409 m^2 for the cycloconverter and VSC respectively [62]. This estimate includes required filtering and compensation.

1.6 Switchgear

Switch gear is used to ensure the safe operation of the electrical system and protect both equipment and life. The main components of switchgear are circuit breakers, relays, fuses, isolators, Fault Current Limiters (FCL), metering equipment and the interconnecting bus bar [50]. Switchgear is classified by the insulating material. On OSS Gas Insulated Switch gear (GIS) is preferred to Air Insulated Switch gear (AIS) due to its compact nature [1]. The recently released ±320 kV DC GIS (circuit breaker not included) from Siemens boasts space saving of up to 70% [63].

1.6.1 Circuit Breakers

The core component of switch gear is the circuit breaker. Circuit breakers must be capable of safely interrupting the maximum feasible fault current within a system quickly enough to avoid damage to the equipment [7].

AC Circuit Breaker (ACCB)

ACCB can be classified based on the arc interrupting medium. Types of ACCBs are oil Circuit Breakers (CBs), minimum oil CBs, air blast CBs, vacuum CBs and gas insulated CBs. Sulfur hexafluoride (SF_6) gas is the most common arc interrupting medium used on OSS [13]. Typically ACCB are available up to 800 kV with a short circuit interrupting capacity of 80 kA [9].

DC Circuit Breaker (DCCB)

Current interruption in DC systems is more severe than AC systems due to the lack of zero crossings in the waveform [12]. Furthermore, fault interruption time requirements are shorter due to the low impedance of DC transmission lines [64]. Currently, no commercial DCCB are available, although successful prototypes such as ABB's HVDC hybrid breaker are awaiting pilot projects [65].
Currently 3 options of DCCB are available: Resonance, Solid-state and Hybrid Circuit breakers. Resonant CB have been successfully tested on point to point HVDC installations but are not appropriate for multi-terminal applications due to insufficiently fast reaction time. They are also limited in current interrupting capability [58]. Solid state CB have no moving parts and can interrupt current and dissipate magnetic energy sufficiently fast, however, the on-state losses are high [12]. A hybrid CB is a compromise. It takes advantage of the favorable breaking ability of semiconductors but includes a parallel high speed mechanical contact to reduce the on-state losses [58].

1.7 Outdoor Insulation

Offshore Wind Energy is harvested with a system composed of wind turbines, cables and converter stations. The collected power is then transmitted to costumers thanks to the main onshore grid.

Along this pathway, there are many applications for indoor and outdoor insulators. The offshore transmission link is usually in HVDC when its length is greater than 100 km. In this case, the offshore station is sometimes provided with composite insulators to withstand the voltage existing between the AC/DC conversion equipment and ground. Indoor insulators are usually maintained clean thanks to the pressurization of the room. Still, insulators are exposed to natural and artificial sources of pollution, e.g. sea, roads, cities and industries.

1.7.1 Selection and dimensioning

The selection and dimensioning of an insulator has the main goal of maximizing the performance of the insulation system over a period of half a century and it is a function of at least six parameters.

$$Insulator\ selection\ and\ dimensioning = f(P1, P2, \ldots, P6)$$

The parameters described in [66] are as follows:

P1 Application depends on the pollution and determines the radial dimension and the orientation of the insulator.

P2 Characteristics of existing insulators developed by manufacturers.

P3 Power System parameters:

- P3.1 AC/DC, maximum system voltage, lightning, switching, temporary overvoltages,
- P3.2 The system's sensitivity to outages, which is high if the system is poor in resilience.

P4 Environment is a function of human and natural instances, and climate, which is a function of atmospheric variables.

P5 Constraints such as:

- Limited insulator choice due to technical requirements
- Cost, caused by budget constraints

- Visual impact to be minimized, in compliance with the law, in more natural landscapes

P6 Field performance monitoring is critical. In fact, it represents a very precious source of data, because it can be used to assess the appropriateness of the insulator choice in the short, medium and long term within a specific spatial and temporal range of selection and dimensioning parameters.

Secondly, it is critical to assess what are the parameters which affect the insulation performance the most. These parameters are called Key Outdoor Insulation Performance Parameters. It is critical to do so, because the combination of different parameter values is infinite, so, to conduct an effective study, it would be helpful to see the interdependencies of the most important ones and the effects on the insulation performance.

1.8 Reactive Compensation

1.8.1 Shunt Compensation

In AC transmission lines, it is required to maintain the desired voltage profile under a fluctuating power demand. Typically, in light load conditions line capacitance can contribute to increase the voltage requiring shunt reactor compensation. On the contrary, under heavy load the shunt capacitive compensation is usually used [67]. Furthermore, subsea HVAC transmission distance is limited due to high cable capacitance. Inductive shunt compensation can be used to increase the range of AC transmission [13].
For shunt compensation the Static Var Compensator (SVC) and Static Synchronous Compensator (STATCOM) are frequently employed. An SVC can supply -300/+600 Mvar at 765 kV with 1.2-2% losses and 98.5% availability. A -100/+300 Mvar unit takes up an area of 20000 m^2 and has a CAPEX of 30-50 k€/Mvar [9]. STATCOMs can supply -200/+200 Mvar at 765 kV with 1.2-2% losses and 99% availability. A -100/+300 Mvar unit takes up an area of 10000 m^2 and has a CAPEX of 50-75 k€/Mvar [9]. Both technologies have an economic lime time of 40 years [9].

1.8.2 Series Compensation

The power transmitted over a line is controlled by changing the series impedance and voltage angle. Through variable series compensation, line im-

pedance can be reduced, power flow controlled and grid stability improved [67].
For series compensation the Fixed Series Capacitor (FSC) and Thyristor Controlled Series Compensation (TCSC) are most frequently employed. A FSC can supply up to 1350 Mvar at 765 kV with negligible losses and 99.5% availability. A 1350 Mvar unit takes up an area of 40000 m^2 and has a CAPEX of 10-20 k€/Mvar [7][9]. TCSCs are suitable for smaller systems having a maximum voltage of 550 V and rated overall power of 493 Mvar. Both technologies have an economic lime time of 40 years [7][9].

1.9 Filters

OWPP are designed using both passive elements such as cables, transformers and capacitor banks as well as active components like wind turbines and HVDC converters. As a result, system resonance and generated harmonics must be carefully considered [7]. A detailed discussion of the more common power quality issues within an OWPP; harmonic resonance and voltage flicker, can be found in [68] and [69]. According to [68], there are primarily 2 techniques employed for mitigating the effects of harmonics. Appropriate design to minimize OWPP harmonics and the use of harmonic filters. There are both passive and active harmonic filters to choose from [7].

1.9.1 Passive filters

Passive filters consist of appropriately sized banks of inductors and capacitors. Passive filters are most common as they are inexpensive, efficient and proven technology. Care must taken to avoid a series or parallel filter to source resonance condition [70]. Passive filters are available up to 550 kV and more than 3 Mvar [7].

1.9.2 Active filters

Active filters combine a Pulse Width Modulation (PWM) frequency controller with a passive filter. Through a feedback controller the desired frequency range of the filter can be dynamically tuned. The main downside to active filters is increased cost. Active filters can be deployed up to 500 kV [7].

1.10 Auxiliary Equipment

1.10.1 Emergency Power System

An OWPP has loads which in the event of a loss of shore power must continue to be energized. These loads include Wind Turbine heating and ventilation, navigation lights and transformer magnetization losses. For a 6 MW REpower turbine emergency power loads amount to 42 kW on average and 193 kVA peak loading [71].
In the case of an emergency, a diesel genset is installed on the OSS. For a 500 MW rated OWPP the genset must provide 5 to 20 MVA. The lower end of the estimate can be achieved if additional reactive compensation is provided and power cycling is performed utilizing the UPS of the wind turbines [71].
A UPS may be placed with the Nacelle of the wind turbine as part of the emergency power system. The UPS in REpower turbines utilizes lead acid batteries and and can supply a 42 kW load for up to 12 hours [71].

1.10.2 Supervisory, Control and Data Acquisition (SCADA)

The SCADA system is the information backbone of the OWPP. Each Turbine, substation and meteorological station is connected to a centralized computer via a fiber optic network. SCADA collects data to give real time system reporting but also has the ability to operate the wind farm in different modes such as frequency or voltage control, power curtailment or reactive power support [7]. A traditional SCADA system usually has the following components [72]:

1. Remote Terminal Unit (RTU)s: are the controllable and monitoring devices (slaves) of any SCADA system, RTUs can have actuators, sensors and communication modules.

2. Master Terminal Units (MTUs): are the servers (masters), they collect data and send commands to the RTUs. A single MTU can control and monitor several RTUs.

3. Communication Infrastructure: is a large-scale and robust communication tool used to transfer commands and data in a SCADA system. This tool can be in different modules or protocols (Local Area Network (LAN), General Packet Radio Service (GPRS), Fiber. . . etc.).

4. The Main Workstation (Operator room): is a large computer with a Human Machine Interface (HMI) used to graphically present and show the SCADA network components (MTUs and RTUs).

In the power industry, SCADA systems can be placed into three categories [73]:

1. Generation: SCADA for power plants and the generation side. It can be used to monitor the bus related measurements (voltage, faults and load), also control the transformers and any circulating current balancing.

2. Feeders (transmission): mainly used to supervise the transmission network to switch links to change power sources, it can also be used to isolate faults using the function of fault detection.

3. End-user (distribution): SCADA is used for more management functions such as billing systems, but is also able to do many load control functions such as load shedding and load scheduling.

General benefits of SCADA systems:

1. Save equipment from breaking down with real-time fault detection.

2. Reduce human risks and manual operation.

3. Provide full supervision of the network to avoid any black-out or outage.

4. Increase the reliability of the grid by automating the process of system recovery after any fault.

5. Increase the accessibility and accuracy of the meter reading process, which benefits the overall efficiency, economics.

6. Improve the sustainability and reliability of future forecasting by storing historical data from different sources.

Nowadays, Energy Management Systems (EMS) and SCADA systems are used to employ the concept of smartgrids and replace traditional grids. Smartgrids provide more flexibility by including Demand-Side Management (DSM) [74, 75]. DSM will increase the capability of the SCADA to achieve:

1. Fewer losses on the grid (controlled demand = no peak loads)

2. Fewer bills for customers (less consumption during peak periods)

3. More environmentally friendly power grid: by controlling the integration of low carbon power generation technologies and reducing CO_2 emissions.

Finding the costs and funds for a SCADA system is one of the nine steps available in [76] to build an interconnection-wide real-time monitoring system, the report explains the cost of a transmission level SCADA and the different sources of funding. It suggests that funding can be obtained from legislatures approbations, directly or tariffs from the asset's owners, or from recovery costs of maintaining the reliability standards.
Also, the report clarified the characteristics that affect the system cost as the following:

1. Network type: AC, DC or hybrid.

2. Monitoring devices: Intelligent Electronic Devices (IED), Phasor Measurements Unit (PMU).

3. Maintenance approach: Preventive, Condition-Based or Corrective.

4. Network Voltage Level: Generation, Transmission or Distribution.

5. Functions and Power Applications System (PAS).

6. Redundancy systems: for higher reliability.

1.11 Offshore Substructures

Offshore substructures are required for both the wind turbines and the OSS. They account for approximately 25% of the total OWPP cost [77]. Six basic types exist: monopile, tripod, tripile, jacket, gravity and floating foundations [78]. the first three are only suitable for turbines and perhaps small collection platforms. The remaining three can be scaled up to accommodate large OSS [58]. Currently monopile and gravity foundations make up 74% and 16% respectively of all Offshore foundations [2]. This is a consequence of near shore, shallow water wind sites being exploited first. As OWPP move farther offshore to deeper water the alternative foundations will become more and more relevant. The most important considerations when selecting a structure are platform size and weight requirements, water depth, wave height, soil and water currents [7].

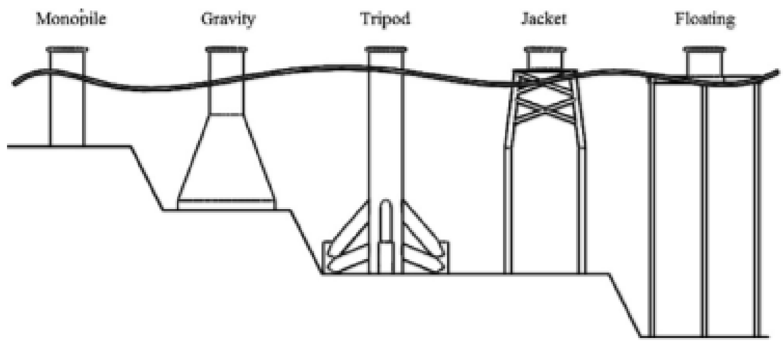

Figure 15: Offshore foundations at relative utilization depths [78]

1.11.1 Monopile Substructures

A monopile substructure is a long steel rod hammered into the seabed [77]. It is suited to depths of 0 to 35 m. Monopiles are simple in design, light weight and versatile but unsuited to large heavy topsides [7]. The largest monopiles installed are 7.8 m diameter and 1302.5 tonne in Veja Mate OWPP [79].

1.11.2 Tripod Substructures

The tripod substructure, is a large tubular steel column supported by 3 tubular steel piles hammered into the seabed. Tripods are a lightweight design good for depths of 20-50 m [7]. A lightweight variation of the tripod is the Slim Tripod Adapted for Rigs (STAR) substructure [77].

1.11.3 Tripile Substructures

The tripile or jacket-monopile substructure, is similar to the tripod substructure except the 3 support piles are secured to the monopile via a jacket of tubular trusses. Tripiles are good for depths of 20-50 m [7].

1.11.4 Jacket Substructures

Jacket substructures consists of 4 to 8 legs connected tubular steal trusses. The legs are secured to piles driven 50 m into the seabed [77]. Jacket substructures are suitable for water depths of 20 to 50 m [7]. They are capable of supporting large topsides such as the 3200 ton BorWin Alpha 400 MW HVDC converter station [58]. Topsides of up to 25000 tons have been supported within the oil and gas industry [58].

1.11.5 Gravity Substructures

A gravity foundation is typical made of reinforced concrete but occasionally steel [77]. Steel structures are more suited to deeper installations up to 25 m [7]. Gravel may be used as a filler to increase weight and stability. Material costs for these substructures are low but installation can be expensive partly due to the need to prepare the sea floor and provide cathodic protection [7], [58]. Gravity structures are capable of supporting any conceivable topside structure within the wind industry [58].

1.11.6 Floating Platform

As sea depth increases the cost of bottom fixed substructures increases rapidly. Around 50 m there comes a break even point where the cost of a floating platform is less expensive [80]. Floating structures rely on buoyancy tanks and an anchoring system to old it in place [58]. Designs of floating structures are generally adopted from the offshore oil industry. Types of floating platforms are semi-submersible, Tension-Leg Platform (TLP) and Spar platforms [77]. An important consideration when co-opting these designs for OWPPs is that MI-type power cable cannot be used with a floating station due to it's lack of flexibility [58].

1.12 Maintenance Approaches

Maintenance is usually monitored by the SCADA system, it shares a big part of the costs. Different approaches can be implemented [81], some of them still under research or not fully employed. However, a combination between them is possible:

1. Preventive or time-based maintenance: this approach depends on the lifespan of the equipment and devices (measuring devices and actuators). Maintenance tests, including parts replacement, are performed before the actual break of the system or equipment. This leads to high costs of the maintenance and it is the price of preventing a fault from actually happening.

2. Corrective maintenance or reactive: this approach is the opposite of preventive, it is activated after a failure occurs. Once the fault is detected, an isolation or recovery process starts in a short time to ensure the continuity of the operation. This approach uses fewer preventative measures. Therefore, it costs less in the maintenance costs but higher in the maintenance performance after the failure occurrence.

3. Condition-based or predictive maintenance: it is a trade-off approach and aims to find the optimal cost of maintenance. This approach monitors the status and health of equipment and detects any possibility of failure which will trigger a maintenance process. Predictive maintenance requires a real-time monitoring system with data collection and analysis functionality. Also, it allows the operator to perform prognostics analysis along with diagnostics analysis.

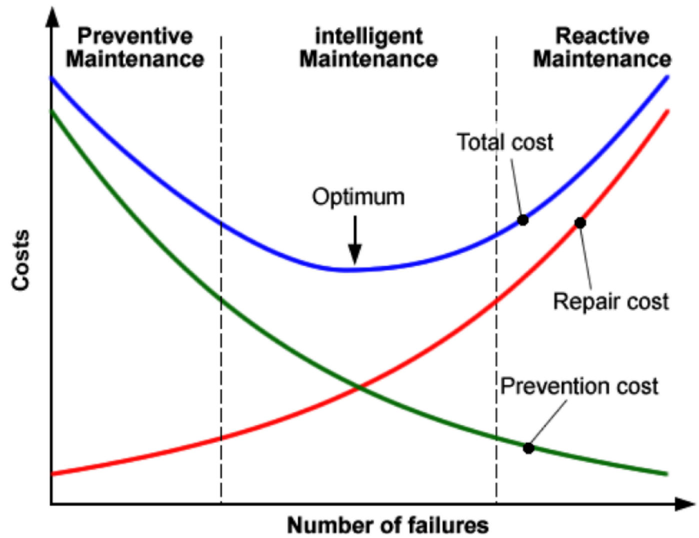

Figure 16: Costs of different maintenance approaches [81]

2 Electrical System Overview

2.1 Introduction

The purpose of the OWPP electrical system is to deliver the power generated by the wind turbines to the PCC efficiently and reliably. It is composed of three major sections. The collection circuit, the OSS or Common Collector Platform (CCP) and the transmission system. Within each of these sections there is a large variety of design decisions to be made such as whether to use AC or DC current, what voltage level or frequency and what level of redundancy is suitable. To account for every conceivable variation is not possible and not the purpose of this section rather to present a thorough yet concise summary of the options available for OWPP electrical system design.

2.2 Offshore system

2.2.1 HVAC and HVDC Transmission

As an OWPP increases in size or moves out to sea there comes a point between 10 to 15 km where the MV used within the collection circuit is no longer cost effective to connect to shore [50]. At this point it becomes necessary to replace the CCP with an OSS equipped with a MV/HV transformer and transmit to the PCC using HVAC. Again as the OWPP moves further from shore, another critical point is crossed, where due to the high capacitance of AC cables, the entire capacity of the cable is used up by the reactive current. This limit can be calculated with (1) [50]. Where $\omega = 2\pi f$, U and I are the rated voltage current of the cable respectively and C' is the cable capacitance taken from the manufacturers data-sheet, and The limit is found to be around 120 km for XLPE type cable [82]. It can be extended with shunt compensation but quickly becomes too costly to justify. In fact, well before the limit, at 87 km for a 600 MW OWPP, connecting with HVDC transmission is the economical choice [83]. As OWPP power increases this distance moves closer to shore.

$$L = \frac{I}{U\omega C'} \tag{1}$$

2.2.2 LFAC Transmission

An alternative to conventional AC 50 Hz and HVDC that has been proposed is LFAC [61]. The most commonly proposed LFAC system would operate at 1/3 of standard frequency (16.7 Hz) allowing for much further HVAC subsea transmission due to substantially reduced cable capacitance [61]. Alternative frequencies have also been proposed. In [84] the optimal frequencies for a 160 MW OWPP at varying distances from shore was found to be 57 Hz, 35 Hz, 23 Hz and 17 Hz for 50 km, 100 km, 150 km and 200 km respectively. Cost estimations have also been performed. In [83] a cost analysis comparing HVAC, LFAC and HVDC found that for a 600 MW OWPP there exists a cost-effective window between 80 and 107 km for LFAC. It was also shown, however, that this window shrinks with increased OWPP power. There are currently no existing OWPP connected via LFAC but a proof of concept laboratory prototype has been successfully demonstrated [83]. Furthermore, LFAC is not new technology. The world's first AC locomotive operated on a 15 Hz, 3000 V three-phase supply and for years 15 kV 16.7 Hz single-phase AC has been used for railway traction systems in Germany, Austria, Switzerland, Norway and Sweden [85].

2.2.3 Collection Circuit

Within the collector circuit AC 20-36 kV is most commonly used [86]. There is no reason this will always be the case. Increasing collector voltage could be beneficial as collector system losses typically constitute the largest percentage of overall system losses [1, 87]. As DC shore connections become more common and DC breakers become commercially available [65], the use of LFAC or DC may become commonplace. A series DC collector system to replace the HVDC converter station is suggested in [88]. It is argued in [89] that DC collection circuits are appropriate with LFAC transmission. The possibilities are not limited to AC, LFAC and DC however. An entirely new architecture for OWPP collector circuits using medium frequency generators and transformers to reduce weight is suggested in [90].

2.3 AC Collection Circuits

The collection circuit's purpose is to transfer the power generated by the turbine generator's to the collection point for transmission to the PCC. There are many feasible collector system topologies. The topologies below are the typical categories of circuits but are not exclusive to each other and can be combined into hybrid circuits if desired. Likewise the number and position collection points is adjustable. According to [91] the optimal solution is likely not one of the standard topologies.

2.3.1 AC topologies

Radial

A radial topology in the cheapest and most utilized collection system. It is formed by stringing the turbines together to the collection point through a single line, with no redundancy. If a failure occurs in a cable all turbines downstream of the fault are cut off. The maximum number of turbines that can be placed per string in determined by the turbine power output and the maximum size of cable available. A big advantage of this layout is the ability to reduce cable size as turbines move away from the collection point [1], [12]. The radial topology is shown in Fig. 17a.

Ring

A ring topology is a variation on the radial layout but with an additional cable forming a loop to the collection point in order to increase reliability. There are three variations of the ring layout:

1. The single sided ring where a cable is connected from the outermost turbine to the collection point to close the loop.

2. The double sided ring where the outermost turbines of two separate radial strings are connected together [1].

3. The multiple ring where the outermost turbines of all separate radial strings are connected together [12].

The ring layout does provide increased reliability, but at a higher cost as additional cable is required and cables must be sized larger to handle current in both directions [1]. The single sided ring has been shown to achieve the lowest losses under both normal and fault operation and a hybrid multiple ring topology with an additional single sided return the most economical when losses are included [12]. The single and double sided ring layouts are shown in Fig. 17b and Fig. 17c.

Star

A star topology is the most reliable of the three but also the most expensive. It is created by running individual connections from each turbine to the connection point. Cable size is substantially reduced but length of cable and installation costs increase, furthermore, the additional switch gear requirements are a major expense [1, 12]. A star topology is shown in Fig. 17d.

2.4 DC Collection Circuits

One of the potential applications of DC/DC converters for DC grids is the offshore wind farm with the DC collection system. The collection system is a medium voltage grid where the wind turbines are connected. Currently AC radial collection systems at 33 kV are mainly used [92]. However, other topologies based on different AC grid configurations, such as ring connection, and even DC collection systems are being studied considering reliability and

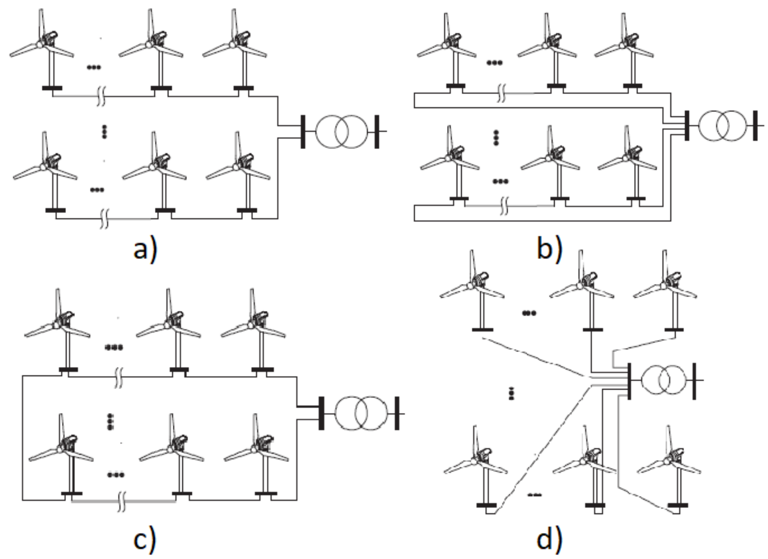

Figure 17: AC collector topologies: a) Radial b) Single sided ring c) Double sided ring d) Star [1]

costs [93]. The different configurations of collection systems are summarized in Fig. 18.
Typically, an offshore wind turbine connected to the AC collection system is integrated with an ac transformer to boost the voltage from low voltage to medium voltage. However, if the DC collection system is applied, the offshore wind turbine should replace the AC transformer with a DC/DC converter to boost the voltage, which is more compact and smaller in size than the AC transformer [16]. If HVDC technology is used to transmit the offshore wind power to the onshore substation, the AC collection system, as shown in Fig. 19a, requires HVAC transformer and the MMC AC/DC converter on the offshore substation platform. Likewise, in the DC collection system as shown in Fig. 19b, an HVDC DC/DC converter is needed on the OSS.

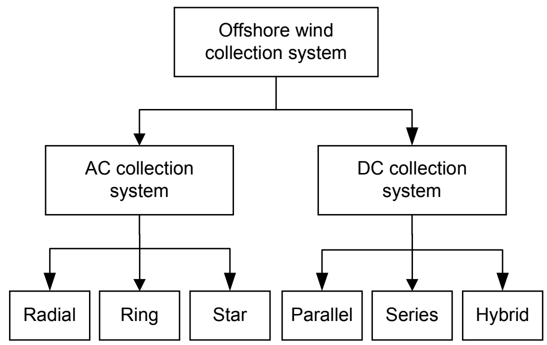

Figure 18: Classification of offshore wind collection system

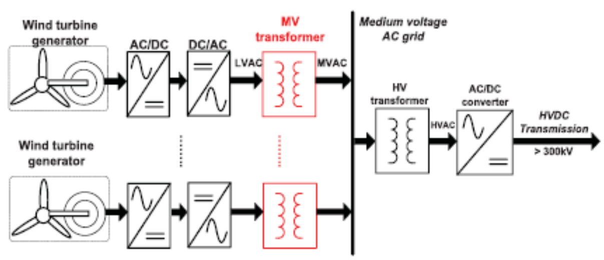

(a) Offshore wind farm with AC collection system

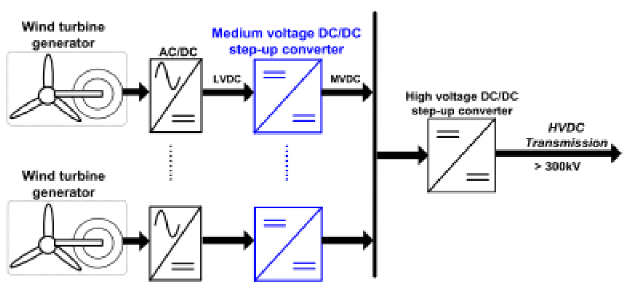

(b) Offshore wind farm with DC collection system

Figure 19: Comparison of AC and DC collection systems [94]

2.4.1 DC Topologies

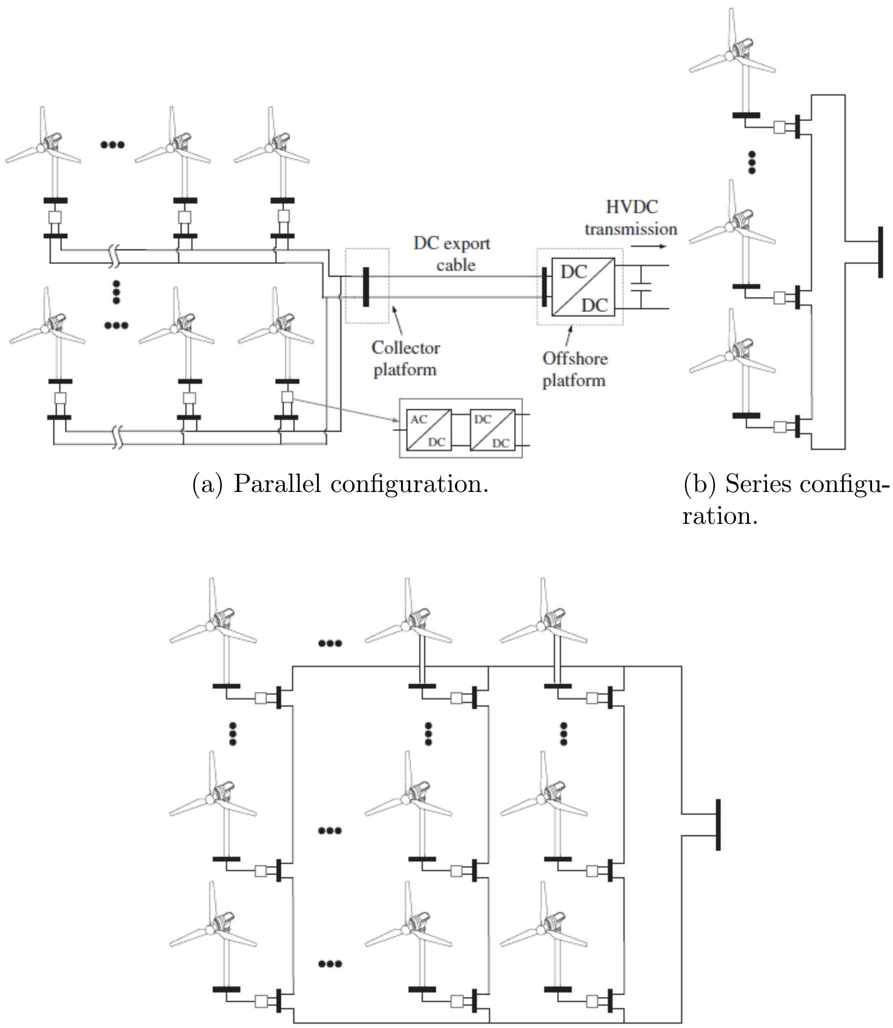

(a) Parallel configuration.

(b) Series configuration.

(c) Hybrid configuration.

Figure 20: Different configurations of DC collection system. (a) parallel configuration; (b) series configuration; (c) hybrid configuration

Although there is no practical offshore wind farm connected with DC connection systems, various configurations of DC collection systems have been proposed in literature. These configurations can be categorized as parallel configuration, series configuration and hybrid configuration as shown in Fig. 20, according to how the wind turbines are connected [44].

Parallel configuration

In the parallel configuration as shown in Fig. 20a, the wind turbines are connected to a MVDC bus in parallel. In this case, the DC voltage of each wind turbine is controlled by the DC/DC converter integrated in the wind turbine. A DC/DC converter OSS is needed for this configuration to boost the MVDC to HVDC. Each wind turbine can work independently, thus the malfunction of one or several wind turbines in the OWPP will not affect the operation of the DC collection system.

Series configuration

A series configuration of the DC collection system is presented in Fig. 20b. The wind turbines are connected in series, thus the currents of each wind turbine are controlled to be constant by regulating the voltage. In this case, the DC collection system can be directly connected to HVDC so an offshore DC substation is avoided, which can reduce the investment costs. However, the drawbacks of this configuration are the difficulties to regulate voltage instead of the current and the oversizing of some electrical components of the OWPP to the maximum power of the entire wind farm. Furthermore, the malfunctioning of one wind turbine can affect the operation of the entire DC collection system.

Hybrid configuration

A hybrid configuration is a mix of parallel configuration and series configuration, so it is also called the series-parallel configuration. In this configuration, several wind turbines are connected into a branch in series, and then the branches are connected to the DC collection bus in parallel, as shown in Fig. 20c. Like the series configuration, the offshore DC substation can be avoided for hybrid configuration, but it features similar drawbacks to the series configuration.

3 Economics and Reliability

3.1 Introduction

As energy production of OWPP is highly variable, infrastructure should be designed for high availability but not necessarily continuous power flow. This differs from standard utility network infrastructure where any interruptions are undesirable. In an OWPP for example, short durations of inoperability due to manual transfer schemes or scheduled maintenance have little affect on system profitability. On the other hand, system repair times are large compared to onshore networks, especially during winter, so unanticipated failure may cause extended outages and have a severe economic impact [95]. In OWPP the cost of space is much higher than on shore. The substructure which supports the OSS and wind turbine platforms contributes approximately 25% to the cost of an OWPP [77]. For OSS this means choosing high cost but compact GIS switchgear and avoiding redundant designs such as ring buses or breaker and a half schemes [95]. Any additional, non essential equipment must contribute sufficiently to energy availability. This methodology may justify, for example, the use of an expensive transformer monitoring system allowing pre-planned scheduled maintenance but not a fully redundant transformer. OWPP electrical system design is based on economics not necessity [95].

3.2 Levelized Cost Of Energy (LCOE)

One of the most important factors allowing for an economic viability comparison of one energy source to another is the Levelized Cost of Energy (LCOE) [96]. European industry has a 2020 target to reduce the LCOE of OWPP from it's current level ranging from 0.119 €/kWh to 0.194 €/kWh down to 0.1 €/kWh [1, 53]. Equation (2) is used to calculate the LCOE [96]. The numerator in (2) is the discounted sum of the lifetime costs of an OWPP. This includes the Initial Investment (LI), the Discounted Operation and Maintenance (DOM), Discounted Fuel Expenditures (DCF) and the expenditures related to CO_2 emissions [96]. All quantities within 2 are their Net Present Value (NPV) equivalents.

$$LCOE = \frac{LI + DOM + DCF + DCCO_2}{E} \quad [\text{kWh€}] \tag{2}$$

3.3 Equipment Cost Functions

3.3.1 Wind Turbine

Initial wind turbine cost (CAPEX) includes, material, transport and installation. For turbines of 2 MW to 5 MW, [97] has derived an expression (eqn: 3) for the material cost derived from real cost data reported in [98]. P_{wt} is the rated power of the wind turbine given in MW. To account for installation and transport it is recommended to add an additional 10% to the turbine manufacturing cost [97].
Several estimates of wind turbine foundation costing have been made [99, 100, 101]. All are for estimates of a monopile foundation as these have been most commonly used [2]. According to a comparative study by [97] against real data, the formulation offered by [101] shown in (4) fits best with average real costs. Where D is ocean depth, d is swept diameter and h is hub height. To account for installation and transport it is recommended to add an additional 50% of the foundation's material costs [97].

$$Cost_{wt} = 2.95 \cdot 10^3 \cdot ln(P_{wt}) - 375.2 \quad [\text{k€}] \tag{3}$$

$$Cost_{fnd} = 320 \cdot P_{wt} \cdot (1+0.02(D-8)) \cdot \left(1+0.8 \cdot 10^{-6} \cdot \left(h \cdot \left(\frac{d}{2}\right)^2 - 10^5\right)\right) \quad [\text{k€/MW}] \tag{4}$$

3.3.2 Cabling

The cost of cabling is related to the length, cross section, voltage level and installation requirements. Equations 5 for AC cables and 6 for DC were presented in [99]. I_{rtd} and U_{rtd} are the cables rated current and voltage respectively. Values recommended for the cost parameters, A_p, B_p and C_p, are found in Table 3. As the original parameters gave values in SEK/km the parameters have been modified to give values in k€/km. An exchange rate of 0.096 €/SEK was used. For Medium voltage (30-36 kV) AC cables a simplified expression as a function of cable cross section (S) was derived by [97] from averaged real cost data and calculations using (5), this is given by (7).
To account for transport to site and installation [97] recommends an additional cost per km of cable between 304 k€- 463 k€ for MV installations up

Table 3: Cost parameters for (5) and (6) [99]

AC				DC		
kV	A_p	B_p	C_p	kV	A_p	B_p $[10^{-6}]$
22	27.264	55.968	6.15	5	-33.216	39.168
33	39.456	57.216	4.1	40	-30.144	5.9328
45	49.536	58.752	3	160	-9.6	1.5744
66	66.048	60	2.05	230	7.584	1.152
132	189.216	20.064	1.66	300	27.456	0.93024
220	305.376	10.56	1.16			

Table 4: Cost estimates of onshore overhead and underground HV lines [97]

	Overhead single line		Overhead double line		Underground cable	
kV	[MVA]	[k€/km]	[MVA]	[k€/km]	[MVA]	[k€/km]
150	210	270	350	410	250	1600
230	340	350	620	450	400	1950

to 30 m depth. The cost per km of collection system cabling consisting of many short (< 1km) jumpers, each of which require lifting and terminating will tend to rise towards the higher end of the range [7]. Collection cabling and associated switch gear account for about 7% of the overall OWPP cost, a high percentage of which is related to installation time. The cost does not significantly change with distance to shore [50]. 720 k€/km is recommended for transport and installation of HV cable [97].
An estimate of land based overhead and underground transmission originally sourced from [102] and compiled by [97] is presented in Table 4.

$$Cost_{acc} = A_p + B_p \cdot exp\left(\frac{\sqrt{3} I_{rtd} U_{rtd} C_p}{10^8}\right) \quad [\text{k€}] \tag{5}$$

$$Cost_{dcc} = A_p + B_p \cdot I_{rtd} U_{rtd} \quad [\text{k€}] \tag{6}$$

$$Cost_{acc} = 0.4818 \cdot S + 99.153 \quad [\text{k€}] \tag{7}$$

3.3.3 Offshore Substation (OSS)

The cost of an OSS is made up of several components. The principle cost comes from the MV/HV transformer, AC/DC converter (HVDC) and platform with foundation. Further to this, switch gear, compensation, SCADA/EMS and the emergency power system should be accounted for [97].
Transformers up to 150 MVA can be estimated by 8 [99], while larger transformers, up to 800 MVA, are better represented by 9 [103]. In both cases P_{rtd} is the rated power of the transformer in MVA. An expression to estimate MV switch gear is provided by 10 [99]. For HV switch gear [97] uses the data originally sourced from [102] and summarized in Table 5. The emergency power system diesel generator can be costed according to (11) [97]. Finally, [99] provides a method of estimating the platform foundation cost using (12). The costing mechanisms of the remaining components, including AC/DC converters, compensation and SCADA/EMS are summarized in Table 6 mostly in the form of average cost/rating.

$$Cost_{tr} = -153.05 + 131.1 \cdot P_{rtd}^{0.4473} \quad [\text{k€}] \tag{8}$$

$$Cost_{tr} = 42.688 \cdot P_{rtd}^{0.7513} \quad [\text{k€}] \tag{9}$$

$$Cost_{sg} = 40.543 + 0.76 \cdot V_{nom} \quad [\text{k€}] \tag{10}$$

$$Cost_{dg} = 21.242 + 2.069 \cdot P_{owpp} \quad [\text{k€}] \tag{11}$$

$$Cost_{ossf} = 2534 + 88.7 \cdot P_{owpp} \quad [\text{k€}] \tag{12}$$

3.3.4 DC/DC Converters

All the analysis of DC/DC converters on reliability, losses and cost is based on calculation, simulation and down-scaled experiments because now there are no DC/DC converters used in the practical situation.
The reliability of DC/DC converter includes the fault isolation ability, fault tolerant ability and galvanic isolation. The fault isolation ability allows the DC/DC converter to work as a DC circuit breaker to isolate faults from the DC grids. All the topologies mentioned above can realize the fault isolation

Table 5: Cost estimates of HV switch gear [97]

		Bus Bar Cost [k€]		Switch Gear Cost [k€]	
kV	Insulation Type	Single Busbar (SB)	Double Busbar (DB)	SB	DB
150	AIS	1780	2350	439	450
	GIS	2650	3280	920	950
230	AIS	1736	2550	637	650
	GIS	2900	3450	1250	1300

Table 6: Average cost/rating of OSS equipment [97, 103]

Equipment	Cost
LCC Converter	0.08 €/VA
Shunt Reactor	2/3 eqn 9
Shunt Capacitor	19 k€/Mvar
SVC	77 k€/Mvar
SCADA/EMS	75 k€/turbine

by specific configuration and control. For HVDC-AT and HVDC chopper, full-bridge submodules are required to block the faults. The fault tolerant ability allows the DC/DC converters to continue to work when some components of the DC/DC converters break down. Redundancy design is required to achieve fault tolerant operation for MMC-DAB and Cascaded DAB, which can guarantee that if several submodules of the converter fail, the converter can still work by replacing the broken submodules with redundant submodules, and the failed submodules will be bypassed. Galvanic isolation may be needed mainly for safety and grounding reasons [23] as is mentioned in Section 1.3.2.

The losses of DC/DC converters mainly consist of switching losses and conduction losses of semiconductors, losses of AC transformers and passive components. In the literature, the losses of semiconductors are mainly considered, especially the switching losses which are related to the switching frequency.

The cost of DC/DC converters is mainly related to the cost of semiconductors and passive components. For OWPP, the cost of constructing a platform is significant, so the cost of DC/DC converters is related to the footprint of DC/DC converters in this situation. The footprint can be reduced by increasing the switching frequency, which brings an increase in losses. Therefore, a tradeoff should be made between losses and costs.

A comparison of the Modular Multilevel DC Converter (M2DC) and the Cascaded DAB is conducted in [25]. It is concluded that the Cascaded DAB is more suitable for offshore DC substations. The efficiency of Cascaded DAB is between 98.9% and 99.2% for most working conditions, while the M2DC shows a poor efficiency of 95.5%. This is because the circulating power in the converter becomes high at high voltage ratios. The investment cost of M2DC is 405000 € while the Cascaded DAB only costs 57100 €. The Cascaded DAB is much cheaper compared to M2DC mainly because of the reduced amount of semiconductor devices. Also, the Cascaded DAB can operate at a higher fundamental frequency reducing the size and cost of capacitors and inductors.

A comparison of MMC-DAB, Cascaded DAB and Cascaded SAB is made for a offshore DC substation in [104] based on semiconductor losses, number of semiconductor modules and cost. The specification of the DC/DC converter is given in Table 7. For this scenario, an F2F MMC requires 6480 semiconductor modules, while the Cascaded DAB only requires only 4416 semiconductor modules. For OSS, the Cascaded SAB can also be considered if only unidirectional power flow from OWPP to grid is needed. Compared to the Cascaded DAB, the Cascaded SAB features a further reduction of the number of semiconductor modules and losses. The application of 3.3 kV and 10 kV noncommercial SiC MOSFET power modules are considered in this comparison. It is concluded that the losses of both MMC-DAB and Cascaded DAB can be reduced if SiC MOSFETs are applied. The MMC-DAB features a higher efficiency due to the relatively lower fundamental frequency, but the Cascaded DAB features a smaller footprint which contributes to the reduction of offshore platform area. It is also highlighted that the key limitation of Cascaded DAB is the high-voltage isolation requirement.

Table 7: Specification of the DC/DC converter in [104]

Input voltage, V_{MVDC}	40 kV
Output voltage, V_{HVDC}	320 kV
Nominal power, P_{dc}	600 MW

The volume and losses of a 30 MW MMC-DAB are discussed in [32]. It is assumed that the cell capacitors can take up approximately 50% of the cell volume of an MMC. By increasing the ac link frequency from 50 Hz to 350 Hz, the capacitance required in the MMC is reduced, which brings significant volume savings. Furthermore, the volume of the AC link transformer is also reduced due to the higher frequency. However, the increase of frequency can cause more switching loss in the MMC. The estimated system efficiency decreases from 98.5% to 97.4% when the frequency is increased from 50 Hz to 350 Hz. Therefore, it is always a tradeoff between system efficiency and volume reduction.

3.3.5 Insulators

The costs of outdoor insulation should be taken into account when developing a OWPP or transmission system.
When building a new HVDC corridor for example, HVDC glsOHL is economically convenient with regards to HVAC Overhead Line (OHL) when the line length exceeds 600-800 [km]. This business case has been carried out in China and Brazil, given the distance between energy resources and big cities. However, if the OHL is already in place, the business case of glsHVAC to glsHVDC conversion may be relevant even with lines ten times shorter. This would increase the probability of transmitting wind power in glsHVDC in the future.

3.3.6 SCADA

Nowadays, the number of traditional power generation plants (large single power stations) is reducing with the introduction of low carbon technologies, such as wind, solar and Distributed Generation (DG). In addition to the environmental benefits of these technologies, they have also improved the power reliability.

However, these low carbon technologies require more investments on the software and hardware tools of SCADA [105], especially on the DC side due to the new complexity in controlling power flow direction [106]. For a reliable AC/DC hybrid SCADA system, modified measuring devices are used on the DC side, along with heavy computational algorithms, and different communication technologies. As a result, the cost of such a system is higher than the traditional AC network SCADA.

The Table below shows the installation cost of two SCADA examples on offshore wind farms:

Table 8: Offshore Wind Farm SCADA system Costs

Project	**Cost**	**Total Capacity**
Nysted wind farm [107] 72 turbines, 2.3 MW each	10.5 M€ C_{st}= 160 k€/turbine	165.6 MW
Offshore Design Engineering (ODE) cost model [108]	1.0 M€ C_{st}= 33.3 k€/turbine	108 MW

Also, [109] has claimed that the cost of a SCADA system per 2.3-3.6 MW turbine is 38.3 k€, including the cost of the communication network. Furthermore [97] has calculated the SCADA cost for an offshore wind farm as proportional to the number of wind turbines, and assumed that the cost of C_{st} SCADA/EMS for a single turbine is:

$$34000 < C_{st} < 75000 \text{ [€/turbine]}$$

Therefore, the estimated cost of SCADA/EMS with n_t turbines is:

$$C_{scada} = n_t C_{st} \quad \text{[€]} \tag{13}$$

For example, for a 30 turbine (2.3 MW each – total 69 MW), the SCADA installation cost can be between 1.02 M€ and 2.25 M€. In general, a SCADA system shares between 1 to 4 percent of the total cost of an AC/DC offshore wind farm project. The annual cost of a SCADA system after installation will be mainly the maintenance cost, which depends on the approach of maintenance.

Despite that SCADA system for wind generations share only a small percentage of the total project cost, it is still higher than SCADA systems for other renewable sources of generation like solar-panel farms. For example, the 3.23 km^2 and 375 k solar panel farm by SunEnergy1 & Duke Energy Renewables [110], argued that the cost of using Wi-fi as a communication medium for the SCADA saved 90% of the total budget of wired communication medium. In addition, the number of sensors per power generation unit is much lower compared to a wind turbine.

3.4 Reliability and Redundancy

Between 2000 and 2004 a Swedish study of wind farm failure found the electrical system accounted for the highest percentage of failures, 17.5% and resulted in 14.3% of plant down time [111]. Failure in OWPP is caused by a large variety of factors including high humidity, salt, water ingression, wave impact, marine vessels and even shifting sea bottoms [112]. Extended unplanned outages are costly as available energy can not be delivered and sold at market [95].

3.4.1 EENS

The EENS due to a failure is calculated using (14) [113]. Where i to N are the components within the system, including switch gear, cables, transformers, generators, converters, etc., q_i is failure rate per year (based on historical data) of piece of equipment i. P_i is the power which can not be delivered due to the failure of component i and is called the Mean Time To Repair $(\text{MTTR})_i$ of component i. The MTTR is the sum of the time taken for failure discovery, failure diagnosis, replacement part acquisition, travel to site and completion of the repair [87].

$$EENS = \sum_{i=1}^{N}(q_i \cdot P_i \cdot MTTR_i) \quad \text{[MWh/year]} \tag{14}$$

A SCADA system allows electric utilities to limit EENS and avoid the Electrical Energy Not Supplied cost, which is a cost that must be paid if fore-casted power is not supplied to customers. It is a function of time [114]. SCADA will improve the uptime of different generation sources, so the shortage of electricity does not stay for long. For example, SCADA will identify the outage location and fault source without waiting for human interaction (call). Also, SCADA provides the operator with several automated options to start a recovery process including isolating the fault and rerouting power direction to save the network from any further damage [72].

3.4.2 Topology and Device Redundancy

Redundancy can be categorized into device redundancy and topological redundancy. These categories can be further divided into redundancy of the collection circuit, platform and transmission system [113]. The purpose of redundancy is to provide an alternative path in which all or a part of expected energy can still be served to market in spite of a component failure. Topological redundancy involves adding additional paths via cabling and switch gear to the collector, transmission or bus bar circuits. While device redundancy involves a design with 1 or more redundant components. For example, most on shore substations are designed with 2 transformers sized at 70% capacity rather than 1 handling 100% of the load [113].

The cost of achieving a reliable SCADA is high. Researches like [115] argued that the reliability of a SCADA system can be increased by replacing the single national SCADA system into one national and one regional size network to increase redundancy. While [116] suggest using several small-scale SCADA systems. However, there is still ongoing research of fully distributed or decentralized [117] SCADA system which in theory could have higher reliability than centralized SCADA [74]. As of today, only centralized SCADA is used because it's compatibility with the current network infrastructure and the cost of changing is very high.

3.4.3 Failure rates and Mean Time To Repair (MTTR)

The failure rates and MTTR of components can be difficult to obtain. Furthermore, MTTR can vary greatly based on location and time of year. MTTR tends to be longer in winter than in summer [118]. Table 9 summarizes values recommended within [112] and [118]. In addition to unexpected failures, equipment also requires a certain amount of scheduled maintenance. Operation and Maintenance (OM) increases with sea depth and distance to shore, a rough estimate of OM is 60000 €/MW/year [119]. Table 10 summarizes recommended maintenance frequency and duration of equipment sourced from [9].

3.4.4 Reliability of HVDC Outdoor Insulation

The reliability of Outdoor Insulation is directly related to its ability to fulfill its purpose, which is withstanding electrical stress even when voltage experiences transients and the conductivity on the surface of insulation is at it's maximum.

In HVDC applications, selection and dimensioning of Outdoor Insulation is mainly determined by pollution, in fact, when wet, it forms a conductive

Table 9: Failure rate and MTTR of common equipment [112][118]

Equipment	Failure Rate	MTTR
MV Breaker on platform	0.025/yr	72 h
MV Breaker elsewhere	0.025/yr	240 h
MV Switch	0.025/yr	240h
LV contactor	0.0667/yr	240h
MV transformer in Nacelle	0.0131/yr	240 h
Transmission Cable	0.015/km·yr	1440 h
Collector Cable	0.015/km·yr	1440 h
Turbine Tower Cable	0.015/km·yr	240 h

Table 10: Maintenance requirements of common equipment [9]

Equipment	Frequency	Duration
AC Transformer	0.2/yr	8h
LCC Converter Station	0.5/yr	168 h
VSC Converter Station	0.5/yr	168 h
AC Breakers	0.067/yr	8 h
STATCOM	0.5/yr	168 h
Static Variable Compensator	1/yr	336 h
Fixed Series Capacitor	1/yr	48 h

layer which degrades the insulator's performance. For this reason, pollution performance will be explained and analysed in its fundamentals, as this can affect the ability to electrically separate the line potential from the ground potential, to avoid short-circuit. Dry pollution is non-conductive, if non-metallic and non-inert, and acquires the hydrophobic property on hydrophobic SiR surfaces. However, wetting of the pollution triggers the dissolution of pollution salts, resulting in a conductive layer. That is when discharge activity begins on the surface of the insulator.

Pollution severity is a function of:

1. The insulator type
2. The electrical application -whether it is AC or DC
3. The nominal voltage of the line
4. The climate
5. The environment

1. The insulator type regards its geometry and material.
2. It has been observed that DC insulation provokes the pollution to be electrically attracted to the insulator, because it is energized, which means it has a stable potential distribution, being able to attract the pollution. Whereas in the AC case the insulators are less covered in pollution, because of the periodical inversion of voltage.
3. In the DC case, the higher is the nominal voltage, the greater the pollution attraction.
4. The climate is defined by many parameters, such as:
    - Temperature
    - Pressure
    - Humidity
    - Rain
    - Snow
    - Ice

- Wind
- Sun radiation

5. The environment is defined by specific human activity or natural circumstances which mainly determine the chemical composition of pollution.

Further in the text, these aspects will be analysed in detail.

One of the main requirements of the insulator is to be able to withstand not only nominal voltage, but overvoltages too in wet-polluted conditions [120] . Others are structural support of the line and long life.

To determine the insulator performance, testing is carried out. When several test methods are used in parallel, the best study results are achieved.

When designing an insulator, product related costs are insulators and test method equipment. The cost of an insulation system can be minimized, considering the possible costs related to the minimization, such as power outages costs and costs due to ageing, etc.

Pollution flashover phenomenon

Pollution flash over consists of six main stages [121]:

1. Dry pollution deposits on the surface of the insulator. If the insulator is SiR made, the hydrophobic property gets transferred to the pollution, because it absorbs the oil released by silicone. At this stage the superficial layer is considerably non-conductive.

2. The wetting of pollution happens because of:

    - Humidity deposit, when the percentage of air humidity is sufficiently high
    - Humidity condensation, which is typical at sunrise
    - Rain
    - Snow and ice melting

    At this stage the pollution dissolves in the water. The result is an electrolyte, which is conductive. Note that these first two steps may be only one, when pollution in the form of a salt is already dissolved in water, e.g. polluted water. Moreover, the pollution may be metallic, in the case of an industrial environment; this kind of pollution needs no water to be conductive, but its degree of conductivity depends on the type of metals it is constituted by and its superficial density distribution on the insulator.

3. The presence of conductive paths allows a current to flow between the two extremities of the insulator, because typically one is at the phase potential and the other at the ground potential. Other extremity potential situations may exist. This current is called *leakage current* because it provokes active power to be lost, since it does not flow all the way to the consumer, being lost on the way.

4. As the leakage current flows, the temperature on the surface rises and the liquid component of the superficial layer evaporates. Some areas dry, thus the current avoids these non-conductive areas going around them. The superficial current density increases at the borders of dry areas, causing more water to evaporate and the dry area to extend in the direction perpendicular to the main leakage current flow direction. The evaporation continues until a *dry band* is formed.

5. At this point the current is not flowing, because of the dry band resistance. However, the voltage, normally applied to the insulator extremities, is now applied on the two borders of the dry band. It is when an arc ignites in air, bridging the dry band, because the air breakdown voltage is lower than the dry band breakdown voltage. The phenomenon is called dry band arcing.

   • In DC conditions, the curved arc in air keeps going, because the voltage is unipolar and sustains the process. Thus, the arc has the time to keep curving upwards, because it is hot plasma.

   • In AC conditions, the voltage keeps reversing, therefore the arc is periodically intermittent. It extinguishes when the voltage applied to the dry band zeroes and it reignites when the voltage overcomes the breakdown value of air.

   The result is that in DC the dry band arcing expands upwards, possibly reaching other surfaces. E.g. it can possibly short-circuit a larger part of the insulator.

In AC the dry band arcing stays closer to the surface, because the arc does not have the sufficient time to expand upwards. It should be possible to experimentally demonstrate that with a very low voltage frequency, the arc would be able to rise in the air more than with a high frequency.

6. More dry bands can be formed as well as other dry band arcs can occur until the complete spanning of the insulator. The final arc, which connects the two insulator extremities is called *flashover*.

The whole phenomenon is graphically displayed in Fig. 21 as follows:

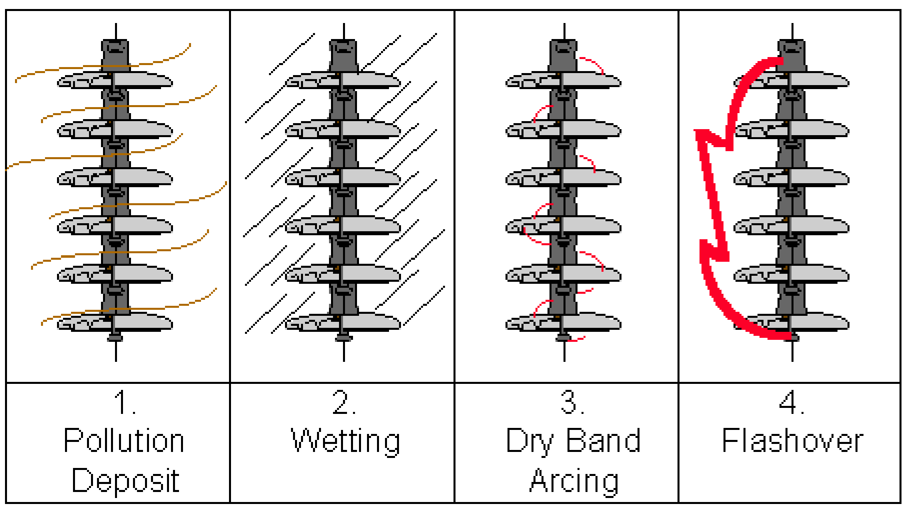

Figure 21: Flashover [120]

Porcelain and glass are hydrophilic materials, so a continuous water layer can easily form, whereas SiR is hydrophobic, so the water stays in the form of droplets. However, the pollution flashover phenomenon follows the same principles for both material types.

Pollution Severity

Definition The pollution severity on the surface of the insulator is expressed in *Equivalent Salt Deposit Density (ESDD)*. In fact, the solution is removed from the insulator surface and its conductivity is measured, then the equivalent salt density having the same conductivity is calculated. This equivalent salt density, expressed in [mg of NaCl/cm^2], is the ESDD of the original pollution layer on the surface of the insulator [122].

Definition *Salt Deposit Density (SDD)* is used when the pollution is NaCl, so there is no need to calculate the equivalent. It is expressed in [mg/cm^2].

Definition The quantity of inert material present on the surface of the insulator is expressed as the *Non-Soluble Deposit Density (NSDD)*. Its quantification is in [mg/cm^2] [122]

Definition The *Site Equivalent Salinity (SES)* [kg/m^3] is the salinity degree of the Salt-Fog test which gives in the lab a leakage current equal to the peak current on the field in wet-polluted conditions.

Pollution Type

(A) Type A pollution is both soluble and non-soluble, respectively measurable with ESDD and NSDD.

(B) Type B pollution is already in the form of electrolyte. One example would be sea spray.

Table 11: Pollution type

Pollution type	Active	**Conductive** 1) metallic deposit close to mining industry: drastic performance drop. Magnetite, pyrite 2) Bird streamer: very high salt content [123, 124, 125]
		Conductive when dissolved 1) gas in solution: hard to detect because measurement provokes evaporation [126]. SO_2, H_2S, NH_3 2) ionic salts: NaCl, Na_2CO_3, $MgCl_2$, $CaSO_4$ (gypsum) 3) Fly ash, cement
	Inert are Tonoko and kaolin	In AC, it has small and indirect influence on the withstand voltage. It retains water, which allows more active pollutant to be dissolved. The impact of the water depends on the quantity of active pollution and its solubility In DC: a) the withstand voltage is very dependent on the inert pollution, under the same ESDD conditions. b) the hydrophobicity of polymeric insulators is affected by the inert pollution (whereas dry active pollution becomes hydrophobic, when deposited on the hydrophobic surface)

Pollution accumulation mechanism

Some pollution is being deposited on the surface of the insulator, some is being carried away or falls from the insulator. The net of the two gives the pollution amount that is being accumulated or reduced.

The three forces, $\mathbf{F}$ [N], which determine the resulting force on a pollution particle close to an insulator are considered in [127, 128, 129, 130] and are:

1. $\mathbf{F}_w$: wind force,
2. $\mathbf{F}_g$: gravitational force,
3. $\mathbf{F}_K$: electric force. This is constituted by two components.
   (a) The electrostatic component, only present in DC energisation
   (b) Dielectrophoretic attraction of neutral particles. Which is negligible compared to the other forces

$$\mathbf{F}_p = \mathbf{F}_w + \mathbf{F}_g + \mathbf{F}_K \tag{15}$$

In AC the electric force is constantly alternating in time, as the electric field reverses, therefore there is not a electrostatic attraction of pollution, but there exists a dielectrophoretic attraction for neutral particles. However, the dielectrophoretic force is negligible with respect to wind and gravitational forces.

In DC there exists an electrostatic force because the electric field is unidirectional [131, 132]. $\mathbf{K}$ is also almost constant in space and time, depending on how low the ripple of the DC voltage is. Thus, pollution, if charged, is attracted to a high electric field region. Moreover, if a neutral particle has a dimension which is great enough, dielectrophoretic attraction towards the insulator happens as well.

$$\mathbf{F}_K = q\mathbf{K} \tag{16}$$

Where the electric field vector $\mathbf{K}$ [V/m] is high in magnitude, the pollution particle, of charge q [C], is attracted with greater force $\mathbf{F}$ [N]. The electric field $\mathbf{K}$ is not easy to calculate analytically in the case of an outdoor insulator, because it depends on the shape of it. The shape is very different from simple geometries like cylinders, but some main concepts need to be remembered. Usually, the high electric field region, which corresponds to the high electric force region, is situated in proximity of sharp corners and needles.

Two research projects demonstrated that increasing the creepage-axial lengths ratio does not necessarily increase the performance of an insulator for the Solid-Layer method [133, 134]. In fact, as seen in [135], there are some recommended limits in the creepage factor, depending on the application type. In the case of composite line insulators, the creepage factor should not exceed 4.3. Moreover, the higher the creepage factor, the most likely it is to overestimate the flashover performance of the insulator.

Maintenance

With regards to maintenance [120], two cases should be distinguished: onshore station insulation and overhead line.

- Onshore station insulation maintenance cost typically regards their cleaning. Station insulators are mostly cleaned once a year with water pumps. The cleaning is carried out in a de-energised condition. The most favorable moment for this operation is summer, since they can dry up quickly and, being summer a dry period in the UK for instance, it is the time of the year in when they would be dirtiest because of minimum natural cleaning.

- Overhead line insulation instead is not designed in a way that would require cleaning, since this operation would be too expensive due to the height of pylons. Only a minority of insulators may be specially treated this way, because of unexpected critical pollution conditions.

3.4.5 Quantifying OWPP Reliability

In order to compare the value of extra redundancy or reliability it is convenient to express system variations in terms of an amount of EENS. The following method to calculate the reliability and resulting ENSS of a OWPP was developed and described in detail by [136]. The main steps of the algorithm are shown in Fig. 22. The algorithm is based on the following assumptions:

- Each component (breakers, cables, transformers, etc.) of the system have only 2 states, functional and non functional, allowing for binary representation.

- All components can be treated independently from each other.

- Each component can carry the maximum current that may be applied to it, ie no overloading can occur. This assumption must be verified through a proper load flow simulation.
- The failure and MTTR remain constant throughout the OWPP lifetime.

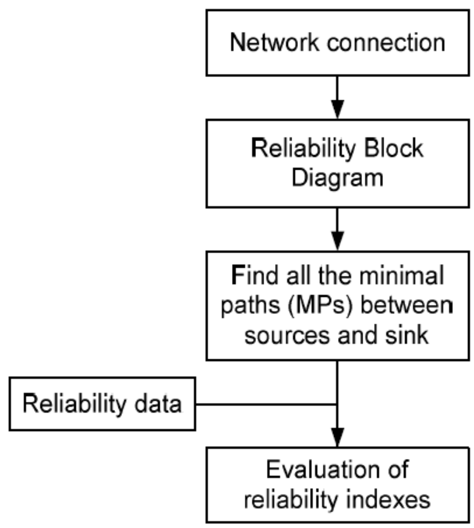

Figure 22: Algorithm to calculate reliability of an OWPP [136]

Reliability Block Diagram (RBD)

Figs. 23a and 23b show the transformation of a collector network in to its equivalent RBD. Figs. 23c and 23d show how the series components of wind turbines and electrical connections are lumped together to simplify the network. The bus-bars are described as perfect nodes which can not fail, as a result the binary status of these nodes will always be 1.

The RBD can be further broken down into N_{ss} sub-systems. Where N_{ss} is the number of wind turbines in the network. Each sub system, shown in Fig. 24, consists of one source and one sink connected by the series and parallel connections forming the paths between them. The perfect bus nodes are neglected.

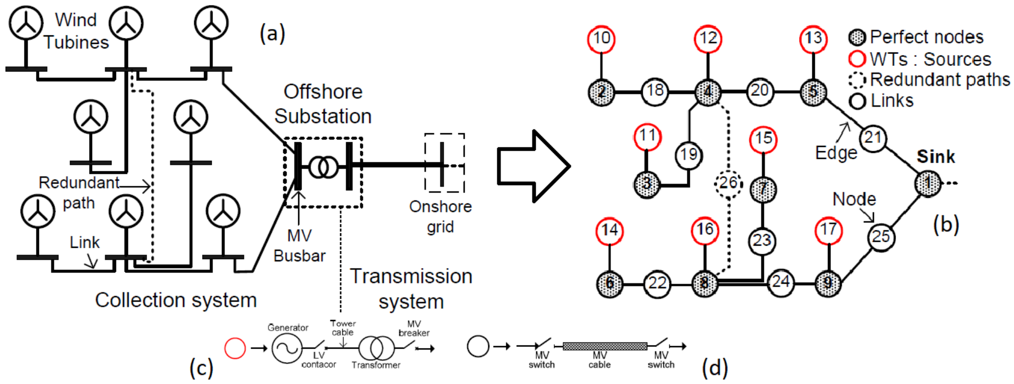

Figure 23: Construction of the RBD [136]. (a) OWPP single line diagram. (b) Block Diagram equivalent of collector circuit. (c) The set of series connected components of a wind turbine. (d) The set of series connected components of electrical connection.

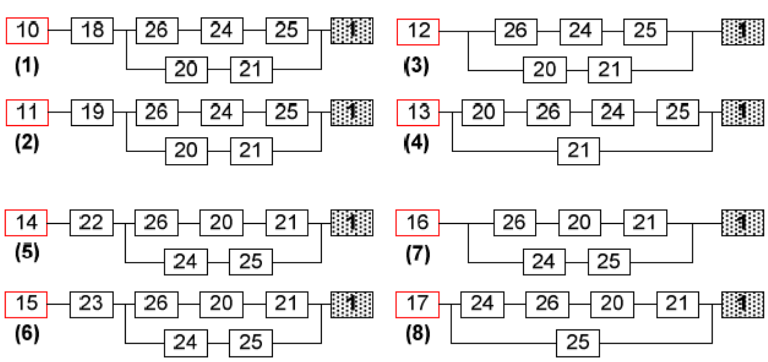

Figure 24: The RBD N_{ss} sub systems [136]

Enumerating Minimal Paths (MP)

Finding all the MPs is the process of describing all the unique paths extending from the sink to each source. This is best understood by viewing the MP tree diagram displayed in Fig. 25. This tree is created by starting at the source node and systematically exposing each new level of nodes. An MP is found when a level exposes a source node. Nodes can appear multiple times within separate MPs, but a path is terminated if a loop occurs, i.e. a node appears twice within the same path. In this example 16 MPs exist.

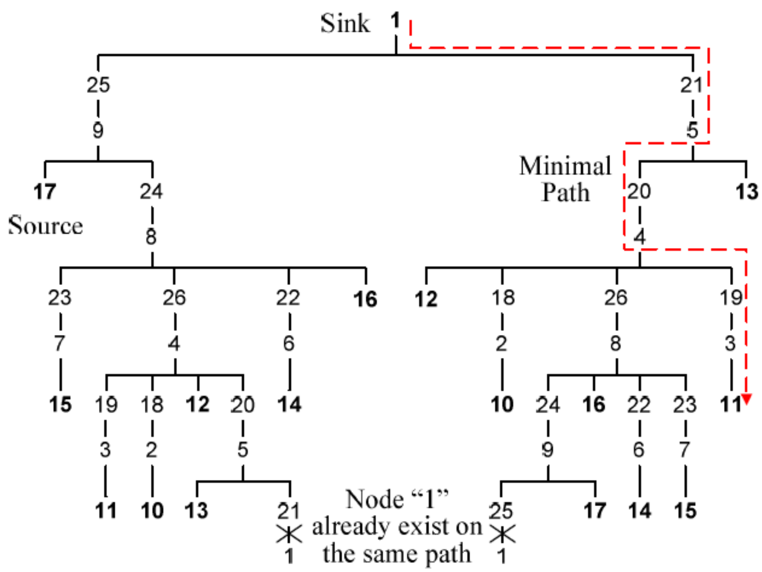

Figure 25: The MP tree for the network RBD [136]

Evaluating Reliability Indices

To begin evaluating the reliability indices, some definitions must be introduced. 17 is the component status vector of the n system components. If $X_i = 1$, component i is functional. Else if $X_i = 0$, component i has failed. 18 is the sub-system j status vector. Sub-system j consists of k MPs. If $\phi_{ss,j}(X) = 1$, sub-system j is functional. Else if $\phi_{ss,j}(X) = 0$, sub system j has failed.

$$X = \left[X_1, X_2 ... X_n\right] \tag{17}$$

$$\phi_{ss,j}(X) = 1 - \left(1 - \prod_{i\epsilon MP_1} X_i\right)\left(1 - \prod_{i\epsilon MP_2} X_i\right)...\left(1 - \prod_{i\epsilon MP_k} X_i\right) \quad (18)$$

The probability that sub-system j is functional at time t is called the availability of sub system j: $A_{ss,j}(A_i)$. A_i is the availability of component i calculated with 19. μ_i (=1/MTTR) and λ_i are the repair and failure rates respectively (Table 9). $A_{ss,j}(A_i)$ is found by replacing X_i with A_i in the expanded form of $\phi_{ss,j}(X)$.

$$A_i(t) = \frac{\mu_i}{\mu_i + \lambda_i} + \frac{\lambda_i}{\mu_i + \lambda_i} \cdot exp(-(\mu_i + \lambda_i)t) \quad (19)$$

Now, EENS can be calculated through (20). Where $P_{wt,j}$ is the power of wind turbine j. Also, the Annual Outage Hours (AOH) can be obtained with 21, and the Equivalent Availability Factor (EAF) with 22.

$$EENS = \sum_{j=1}^{N_s} (1 - A_{ss,j}) \cdot P_{wt,j} \cdot 8760 \quad \text{MWh/year} \quad (20)$$

$$AOH = \frac{EENS}{\sum_{j=1}^{N_s} P_{wt,j}} \quad \text{h/year} \quad (21)$$

$$EAF = 1 - \frac{AOF}{8760} \quad \text{pu} \quad (22)$$

For large systems, the expanded form of $\phi_{ss,j}(X)$ is difficult to find. When this is the case, it is recommended that the simplification shown in Fig. 26 be applied. The simplification assumes all parallel blocks are perfect blocks and omitted. This assumption only introduces error when two parallel components are in a failed state concurrently, a rare occurrence. The simple approximation of $A_{ss,j}$ shown in (23) is then applied. Where U is the set of components in the new simplified sub system. Within [136] this assumption is shown to provide results close to the exact solution.

$$A_{ss,j} = \prod_{i\epsilon U} A_i \approx 1 - \sum_{i\epsilon U} (1 - A_i) \quad (23)$$

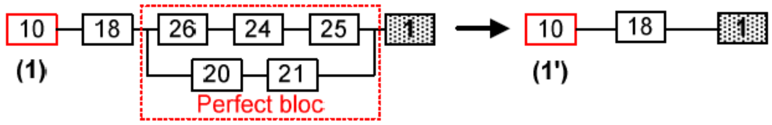

Figure 26: Simplifying assumption for parallel paths in large systems [136]

3.5 Economics of OWPP Losses

There are 3 types of losses to consider: fixed losses, variable losses and EENS. Fixed losses are mostly due to transformer excitation and conductor dielectric losses. They are constant under varying load. Variable losses are ohmic losses (I^2R) mostly within the cables and transformers [87]. These losses vary with output. Finally, EENS is available energy that could not be delivered to market due to a failure or limitation of the design [95]. Losses must be accounted for in each component of the OWPP.

In DC systems the largest source of losses comes from the converter while in AC systems from the cabling [119]. Collector system cable losses typically form the largest percentage of total OWPP losses [87]. Knowledge of the following is necessary to determine collector system losses: the wind turbine ratings, the operational power factor, the cable gauge, length, and the collector configuration itself. OSS and wind turbine generator transformer loss include both copper and core losses. These are best determined using representative data from similar transformers. As core losses are present even during zero production, transformers with low loss amorphous cores may be desirable [87]. The reactive power compensation system has both no-load and on load losses. Typically, the different components of a hybrid compensation system must be treated individually. Loss calculations are based on expected on time of capacitors and reactors and average reactive power output levels [87]. It is convenient to represent these losses as a NPV equivalent.

3.5.1 Fixed Losses

A method utilized by US utilities to translate fixed losses into an initial CAPEX is the A factor [137]. The A factor is a value in €/kW which represents a CAPEX resulting in a 1 kW reduction in fixed losses. Design decisions can then be accepted or rejected on whether the rate of return associated with the A factor is desirable or not. The A factor is calculated by solving for A, in (24) to (26) [95]. Table 12 summarizes the variable definitions. The calculation is based on US tax law and pricing mechanisms however, the equations can be adapted to European policy.

$$PV_{cap} = PV_{rev} \tag{24}$$

$$PV_{cap} = A - A \cdot T \cdot \sum_{n=1}^{life} \left[\left(\frac{p}{f}\right)_n^i \cdot D(n) \right] + A \cdot \left(\frac{p}{a}\right)_{life}^i \cdot (1-T) \cdot P \tag{25}$$

$$\begin{aligned} PV_{rev} = \left(\frac{p}{a}\right)_{life}^i \cdot \left[H_0 \cdot C_{ep} + (8760 - H_0) \cdot C_{ew} + C_{dem} \right] \cdot (1-T) \\ + \left(\frac{p}{a}\right)_{life\_ptc}^i \cdot (8760 - H_0) \cdot C_{ptc} \end{aligned} \tag{26}$$

3.5.2 Variable Losses

Variable losses or the B factor are calculated in a similar manner to the A factor using (24). PV_{cap} is calculated in the same manner but B is substituted for A in (24). PV_{rev} is different, however, as variable losses vary with production. The calculation of the B factor's PV_{rev} is given by (27) and (28). Table 12 summarizes the variable definitions. Like the A factor, the B factor provides a value in €/kW which is the incremental CAPEX at a specified rate of return which results in a 1kW reduction in variable losses [95].

$$PV_{rev} = \left(\frac{p}{a}\right)_{life}^i \cdot 8760 \cdot K_{loss} \cdot (1-T) + \left(\frac{p}{a}\right)_{life\_ptc}^i \cdot 8760 \cdot K_{loss} \cdot C_{ptc} \tag{27}$$

$$K_{loss} = \frac{1}{8760} \int_0^{8760} \overline{P(t)}^2 \cdot dt \tag{28}$$

3.5.3 EENS Losses

EENS, as explained in 3.4.1, is the energy which was available to sell but could not be transferred to the market due to some failure or limitation

Variable	Definition	Variable	Definition
PV_{cap}	Present value of a CAPEX of type A,B or C	PV_{rev}	Present value of the impact on net revenue of a CAPEX of type A,B or C
A	initial capital cost equivalent of no-load losses-A factor (€/kW)	B	Cost equivalent of load-dependent losses-B factor (€/kW)
C	Cost equivalent of EENS-C factor (€/kWh/year)	H_0	Hours/year with no generation
$\left(\frac{p}{f}\right)_x^y$	Present value of a year x future cash flow under compound interest y	$\left(\frac{p}{a}\right)_x^y$	Present value of a year 1 to x set of uniform cash flows under compound interest y
D(n)	Tax depreciation in year n of the capital asset	i	Desired return on investment after tax
$life$	OWPP economic lifetime	P	Property tax rate
T	Income tax rate	C_{ew}	Selling price of electricity
C_{ep}	Cost of purchased electricity (€/kWh)	C_{ptc}	Wind generation production tax credit (€/kWh)
C_{dem}	Demand (capacity) charge of purchased power (€/kW$_{peak}$/year	$life\_ptc$	Duration of wind generation production tax credit (€/kW$_{peak}$/year)
K_{loss}	Average variable losses divided by losses at rated production	$\bar{P(t)}$	Hourly per-unit power output of the OWPP. Refer to Fig. 27
K_{cap}	OWPP Capacity factor		

Table 12: Variable definitions of (24) through (29) [95]

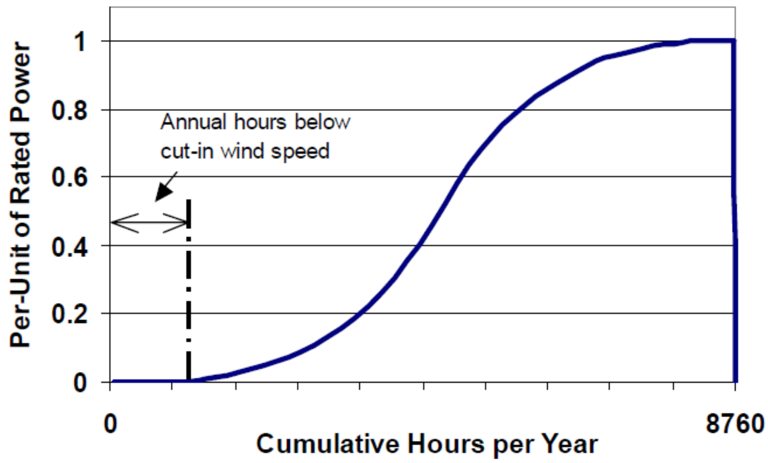

Figure 27: Example of Hourly per-unit power output of an OWPP ($\overline{P(t)}$). [95].

of the design. This could be due to equipment failure, maintenance or a lack of capacity. The C factor is a useful method for quantizing the EENS. Like the A and B factors (24) and (25) are used substituting A with C. To calculate P_{rev} (29) is used. Table 12 summarizes the variable definitions. The C factor provides a value in €/kWh/year which is the incremental CAPEX at a specified rate of return which results in a 1 kWh/year reduction in lost energy production [95].

$$PV_{rev} = \left(\frac{p}{a}\right)^{i}_{life} \cdot 8760 \cdot K_{cap} \cdot C_{ew} \cdot (1-T) + \left(\frac{p}{a}\right)^{i}_{life\_ptc} \cdot 8760 \cdot K_{cap} \cdot C_{ptc} \quad (29)$$

3.5.4 Sizing and redundancy calculations

Typically sizing of equipment is done purely based on electrical requirements such as ampacity, short ciruit levels and thermal limits [87]. Of course these conditions must be satisfied by any design but sizing in this manner does not take into account the economics of losses. An alternative approach is using the A and B factors. This allows equipment to be sized to their economic optimum while still satisfying all electrical constraints. Equation (30) shows how this is done in the case of a transformer [95].

Furthermore, by including the C factor the viability of redundant equipment configurations can be quantified ((31)) [95]. This calculation requires the calculation of E_{Loss}. E_{Loss} is the energy lost during the stopage. E_{Lost} is a function of the MTTR and the OWPP capacity factor. To demonstrate, (32) shows how to analyze whether an OSS should have 1 full size or 2 half size transformers. This comparison requires the additional calculation of the OWPP constrained capacity factor K_{ccf}. K_{ccf} is calculated in the same manner as K_{cap}, but with an upper limit of generation is applied as shown in Fig. 28. All variable definitions are summarized in Table 13.

$$Cost_{size} = Cost_{init} + A \cdot P_{nl} + B \cdot P_{ll} \cdot \left(\frac{P_{full}}{P_{np}}\right)^2 \tag{30}$$

$$Cost_{redund} = Cost_{size} + C \cdot E_{Lost} \tag{31}$$

$$E_{Lost} = \begin{cases} P_{owpp} \cdot MTTR \cdot K_{cap} & : 1\ Xformer \\ P_{owpp} \cdot MTTR \cdot \left(K_{cap} - K_{ccf}\right) & : 2\ Xformers \end{cases} \tag{32}$$

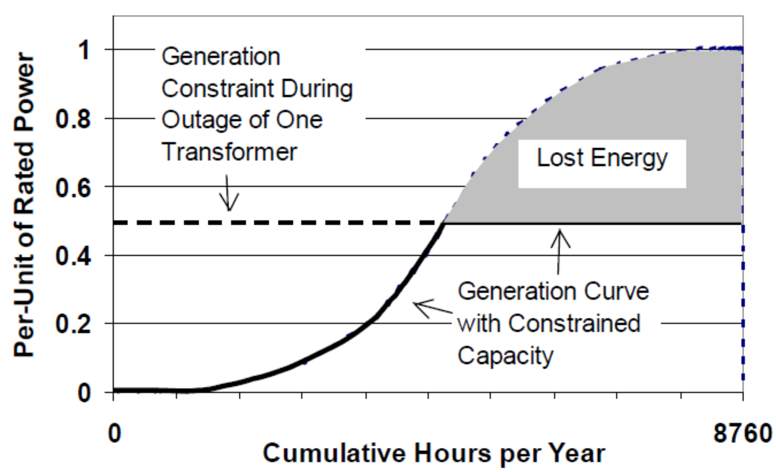

Figure 28: Example OWPP graph used to calculate K_{ccf} [95].

Table 13: Variable definitions of (30) through 32 [95]

Variable	Definition	Variable	Definition
$Cost_{init}$	transformer CAPEX of material and installation	P_{nl}	Transformer no-load loss (kW)
P_{ll}	Load loss at nameplate rating (kW)	P_{full}	Transformer loading at full generation output (kVA)
P_{np}	Transformer nameplate rating (kVA)	E_{Lost}	Energy lost during transformer outage (kWh)
P_{owpp}	Rated power capacity of OWPP (kW)	K_{cap}	OWPP capacity factor
$MTTR$	Mean time to repair asset	$K_{c}cf$	Constrained OWPP capacity factor. Fig. 28

4 Optimization

4.1 Introduction

The optimization of OWPP can be divided into macro and micro sitting (optimal farm and turbine placement) and electrical layout optimization. OWPP optimization discussed within assumes farm and turbine position has been previously optimized and is fixed, focusing only on electrical layout optimization. OWPP electrical optimization is an Nondeterministic Polynomial time (NP) hard problem as the objective function and constraints are nonlinear, non convex, multi variable and multi restrictive [138]. Although, OWPP optimization is still a young field of study it shares many commonalities with Generation capacity and Transmission Expansion Planning (TEP) optimization which have both been extensively investigated [139]. Similar to TEP, OWPP optimization has an investment phase and operational phase with stochastic inputs (wind regimes and component failures) which must satisfy power flow constraints [140].

4.2 Formulation

Generally two categories of optimization formulations have been investigated; classical and non-classical. The classical formulation requires a strict mathematical formulation of an objective function which can be restrictive, however the optimal solution can be guaranteed. The formulation of the objective function and associated constraints can allow for Linear Programming (LP), Mixed Integer Programming (MIP), Mixed Integer Quadratic Programming (MIQP), Mixed Integer Non-Linear Programming (MINLP) or Geometric Programming (GP). Popular algorithms and solvers that can be applied to these types of problems are shown in Table 14. Non-classical methods allow for a more flexible formulation that can be applied afford-ably to very large and complex problems but at the expense of guaranteed optimality. Non-classical optimization methods applied include, heuristic, meta-heuristic and hybrid. The most common non-classical approach is the Genetic Algorithm (GA) [140].

Both classical and non-classical methods have their advantages and formulation selection should be done in conjunction with modeling choices. In [140], it is recommended to avoid pure heuristics, LP and GP and choose either a meta-heuristic or MIP or MIQP coupled with stochastic problem decomposition techniques, particularly benders decomposition. With any chosen method it is advisable to use scenario reduction and aggregation techniques in order to reduce problem size and achieve acceptable convergence times.

Table 14: Popular Algorithms and Solvers used for Classical methods [140].

Method	Algorithms (SOLVER)
LP	Simplex, Interior point method
MIP/MIQP	Branch and Bound, Branch and Cut (CPLEX)
MINLP	Reduced Gradient method (MINOS)

4.3 Objective Function

The electrical layout problem consists of finding the optimal number, capacity and configuration of the electrical equipment that minimizes the life cycle system costs. This includes the initial investments, losses, maintenance and EENS due to unavailability over the OWPP lifetime. The objective function is shown in (33) [141]. The optimal solution should return the following:

- Collector circuit voltage level and frequency (AC, LFAC or DC).
- Transmission system voltage level and frequency (AC, LFAC or DC).
- The connection topology of the collector circuit including wind turbine grouping, OSS connection and any redundant paths.
- Number and location of OSS and CCP.
- The connection topology of the transmission system including the number of cables, sizes, connections among OSS(s) and the PCC(s).
- Type, rating and location of all cables, switch gear, transformers, converters, compensation equipment and emergency power generator.

$$C_{lcsc} = C_{inv} + \sum_{i=1}^{life} \left(C_{loss,i} + C_{main,i} + C_{eens,i} \right) \tag{33}$$

4.3.1 Constraints

Any electrical design must satisfy the power flow equations. This means that under normal operation no overloading of equipment may occur. As AC submarine cables have a much higher capacitance compared to overhead lines, the effect of reactive power on voltage magnitude cannot be neglected and an AC power flow method must be utilized [141]. Furthermore, the Transmission System Operators (TSO) has grid requirements which may place constraints on the solution. For example, European Network of Transmission System Operators (ENTSO)-E Article 20(3) requires unity Power Factor (PF) be supplied to the MV bus of the collector transformer and UK grid code C.6.3.2 specifies a V-Q envelope (Fig. 29) for reactive power control at the PCC [142]. Any design must have the ability to satisfy all grid compliance requirements. Although it is not essential, it is logical that equipment type and size satisfy those commercially available and that, due to practical feasibility, underwater cables should not cross [138].

4.3.2 Reducing Search Space

Modeling of the electrical system is very complex. Previous research has attempted various methods of simplification. According to a study by [143],

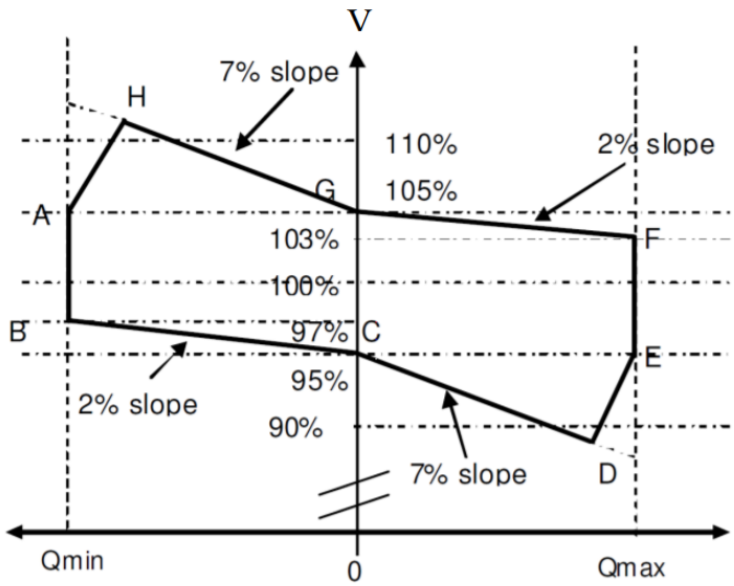

Figure 29: V-Q power envelope (CC.A.7.2.2) [142].

the electrical system can be divided into three subsections and each treated independently. Subsection 1 is the collection circuit which consists of all equipment from and including the wind turbines up to the OSS or CCP connection. Subsection 2 is all equipment located on the OSS or CCP. Subsection 3, the transmission system, encompasses all equipment from the OSS or CCP connection right up to the PCC.

Making Assumptions

Various assumptions to reduce the search space can be found throughout the literature. In [1] the collector circuit was limited to radial configurations and the number of connections per turbine to 2. Meshed DC grids have been ignored or as in [138] the DC solution excluded entirely and MV/HV voltage levels imposed. The stochastic nature of wind can been limited to speed only or ignored entirely [140]. A similar approach has been taken with component failure. The possible number and location of OSS(s) and CCP(s) is limited to 2 and connections between turbines restricted to direct neighbors in [144]. A common assumption is to restrict equipment ratings and types to those commercially available as in [138].

All assumptions have the advantage of reducing search space but must be made with caution as they run the risk of excluding the true global optimal. In [91] it was shown that the true optimal solution is rarely among the standard configurations. While [138] demonstrated the benefit of the free evolution of the number and positions of the OSS(s). The inclusion of stochasticity was proved beneficial by [144]. As wind farms move further from shore the exclusion of a DC solution seems less valid.

Scenario Aggregation and Reduction

Reducing the dimension of the problem as much as possible through scenario reduction and aggregation is essential [140]. The purpose is to reduce the search space by eliminating designs that are outside predefined criteria prior to full optimization. Scenario aggregation involves grouping similar solutions into a single representative sample and is described in detail within [145]. Scenario reduction involves eliminating scenarios that don't satisfy specific criteria. To illustrate, Fig. 30 shows a method for shortlisting designs developed by [119].

4.4 Power Flow

It is a constraint of the problem that no component may be subjected to a load under normal operating conditions which exceeds it's rated capacity. To ensure this, a power flow calculation is performed. With Sub-sea cabling an AC power flow must be used as cable reactance is substantially higher than in overhead lines [141]. A further complication arises with the introduction of a meshed AC/DC system. The in house developed open source software PowerModelsACDC available at [146] and described in detail for an optimal power flow problem here [147] is believed to nicely meet the requirements.

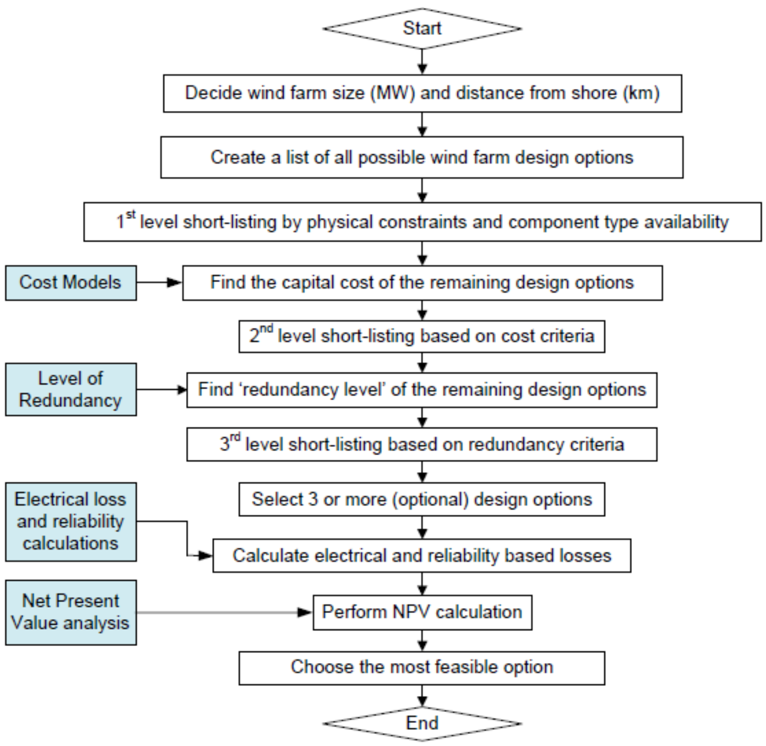

Figure 30: Algorithm for Scenario reduction [119].

5 Conclusions

5.1 DC/DC Converters

The topologies of DC/DC converters for OWPP and HVDC grids have been reviewed. The calculation and analysis of the cost and reliability of DC/DC converters has also been studied. First, the characteristics of DC/DC converters have been summarized considering the advantages and disadvantages of each topology. The requirements of the DC/DC converter for OWPP DC collection system have been considered. Also, the reliability of DC/DC converters has been discussed, including the fault isolation ability, fault tolerant ability and galvanic isolation. Besides, the cost and losses of DC/DC converters have been introduced. Different topologies of DC/DC converters have been compared based on losses, investment cost and footprint. Since there are no DC/DC converters used in the practical situation now, all the analysis of DC/DC converters for HVDC grids has been based on calculation, simulation and downscaled experiments. However, the analysis of reliability, cost and losses is very important for the future designing of DC/DC converters and DC grids.

5.2 SCADA

An introduction to SCADA system has been presented, including the structure of the system, the categories of SCADA based on networks and the main benefits. Further details of the environmental aspect and the funding resources have been mentioned.
The criteria that affect the cost of establishing a SCADA system have also been listed. Despite that the cost of SCADA systems are not fully available to the public, SCADA for an OWPP AC/DC hybrid networks is assumed to be calculated using a statistical unit multiplied by the number of wind turbines in the OWPP.
In addition, the contribution of SCADA in reducing the EENS has been explained. And, the relation between the centralized and distributed SCADA systems with the reliability has been discussed.

5.3 Outdoor Insulation

The main parameters affecting the reliability and the cost of outdoor insulation have been reviewed in detail. Focus has been dedicated to the pollution flashover phenomenon which is the starting point of the selection and dimensioning of insulators on which cost is directly dependent.
The identification and characterization of the type of environment is critical, typically for HVDC onshore substations close to coast, since marine salt highly affects the insulation performance.
HVDC energization is not well known and documented in scientific literature, moreover composite insulators are relatively new. Therefore, the development of new solutions and standard procedures to test such indispensable equipment need to be investigated in the future work.
At the present state of the electricity network, HVDC outdoor insulation is used for Offshore Wind Farms for the onshore substation only and when the connection cable is longer than typically 100 [km]. Insulation is used on offshore platforms in some cases, but does not suffer from pollution problem. Whereas Outdoor Insulation for OHL, which would constitute the DC grids research section of InnoDC, has only been used in a very small number of countries, such as China, Brazil. However, this Deliverable focuses on the application of outdoor insulation for Wind applications strictly.

5.4 Economics/Reliability

Methods to calculate the cost and reliability of OWPP have been considered. First cost models for individual components have been discussed. The presented cost models account for both materials and labor. Second, the concepts of reliability and redundancy have been introduced and a method to quantize reliability presented. Third, lifetime fixed and variable losses as well as EENS due to planned and unplanned downtime have been explained and calculated via utilization of the A, B and C factors. The calculation of the A, B and C factors simultaneously demonstrates how to find a NPV equivalent value. Combining the above concepts together, makes it possible to calculate the LCOE. The LCOE is a powerful quantity as it allows not only for a particular OWPP design to be compared to another but also to entirely different sources of energy.

References

[1] Mikel de Prada Gil. *Design, operation and control of novel electrical concepts for offshore wind power plants.* PhD thesis, UPC Universitat Politechnica de Catalunya, 2014.

[2] European Wind Energy Association. Deep water, the next step for offshore wind energy. Technical report, July 2013.

[3] M. Damen J.T.G. Pierik P.Bauer, S.W.H. de Haan. Offshore wind farms electrical configurations - a case study. Technical report, Netherlands Energy Research Foundation, 2003.

[4] Lena Max. *Design and control of a DC Collection Grid for a Wind Farm.* PhD thesis, Department of Energy and Environment, Chalmers University of Technology, 2009.

[5] *Wind power in power systems.* Wiley, Chichester, 2005.

[6] C.R. Meyl J.T.G. Pierik P.Bauer, S.W.H. de Haan. Evaluation of electrical systems for offshore windfarms. Technical report, Netherlands Energy Research Foundation, 2003.

[7] Antonios Cutululis N. Das, K. Offshore wind power plant technology catalogue - components of wind power plants, ac collection systems and hvdc systems. Technical report, 2017.

[8] 9 - cables. In E.A. Reeves, editor, *Newnes Electrical Pocket Book (Twenty-first Edition)*, pages 169 – 188. Newnes, twenty-first edition edition, 1992.

[9] Grid innovation online technology database. http://www.gridinnovation-on-line.eu/Technology-Database.

[10] G.J. Smith P.Gardner, L.M. Craig. Evaluation of electrical systems for offshore windfarms. Technical report, Garrard Hassan and partners.

[11] An introduction to high voltage direct current (hvdc) subsea cables systems. Europa Cable, www.europacable.com.

[12] SJ Shao and Vg Agelidis. Review of dc system technologies for large scale integration of wind energy systems with electricity grids. *Energies*, 3(6):1303–1319, June 2010.

[13] Sthitadhee Sarkar. Transmission options for offshore windfarms in scotland. Master's thesis, Department of Mechanical and Aerospace Engineering Power University of Strathclyde, January 2012.

[14] Superpower-inc, hts transmission cable. http://www.superpower-inc.com/content/hts-transmission-cable.

[15] W.L. Kling, R.L. Hendriks, and J.H. Den Boon. Advanced transmission solutions for offshore wind farms. pages 1–6. IEEE, July 2008.

[16] K. Musasa, N. I. Nwulu, M. N. Gitau, and R. C. Bansal. Review on DC collection grids for offshore wind farms with high-voltage DC transmission system. *IET Power Electronics*, 10(15):2104–2115, 2017.

[17] M. Forouzesh, Y. P. Siwakoti, S. A. Gorji, F. Blaabjerg, and B. Lehman. Step-up DC –DC converters: A comprehensive review of voltage-boosting techniques, topologies, and applications. *IEEE Transactions on Power Electronics*, 32(12):9143–9178, December 2017.

[18] R. W. A. A. De Doncker, D. M. Divan, and M. H. Kheraluwala. A three-phase soft-switched high-power-density DC/dc converter for high-power applications. *IEEE Transactions on Industry Applications*, 27(1):63–73, January 1991.

[19] A. R. Prasad, P. D. Ziogas, and S. Manias. Analysis and design of a three-phase offline DC-dc converter with high-frequency isolation. *IEEE Transactions on Industry Applications*, 28(4):824–832, July 1992.

[20] X. Li and A. K. S. Bhat. Analysis and design of high-frequency isolated dual-bridge series resonant DC/dc converter. *IEEE Transactions on Power Electronics*, 25(4):850–862, April 2010.

[21] B. Zhao, Q. Song, W. Liu, and Y. Sun. Overview of dual-active-bridge isolated bidirectional DC –DC converter for high-frequency-link power-conversion system. *IEEE Transactions on Power Electronics*, 29(8):4091–4106, August 2014.

[22] G Belverde, A Galluzzo, M Melito, S Musumeci, and A Raciti. Active voltage sharing of series connected strings of igbt devices in bridge applications. In *Industry Applications Conference, 1998. Thirty-Third IAS Annual Meeting. The 1998 IEEE*, volume 2, pages 817–824. IEEE, 1998.

[23] J. D. Paez, D. Frey, J. Maneiro, S. Bacha, and P. Dworakowski. Overview of DC-dc converters dedicated to HVDC grids. *IEEE Transactions on Power Delivery*, page 1, 2018.

[24] Wu Chen, Xinbo Ruan, Hong Yan, and K Tse Chi. Dc/dc conversion systems consisting of multiple converter modules: stability, control, and experimental verifications. *IEEE Transactions on Power Electronics*, 24(6):1463–1474, 2009.

[25] S. P. Engel, M. Stieneker, N. Soltau, S. Rabiee, H. Stagge, and R. W. De Doncker. Comparison of the modular multilevel DC converter and the dual-active bridge converter for power conversion in HVDC and mvdc grids. *IEEE Transactions on Power Electronics*, 30(1):124–137, January 2015.

[26] M Amin Bahmani, Torbjörn Thiringer, Ali Rabiei, and Tarik Abdulahovic. Comparative study of a multi-mw high-power density dc transformer with an optimized high-frequency magnetics in all-dc offshore wind farm. *IEEE Transactions on power delivery*, 31(2):857–866, 2016.

[27] B. Zhao, Q. Song, J. Li, Y. Wang, and W. Liu. High-frequency-link modulation methodology of DC –DC transformer based on modular multilevel converter for HVDC application: Comprehensive analysis and experimental verification. *IEEE Transactions on Power Electronics*, 32(5):3413–3424, May 2017.

[28] Stephan Kenzelmann, Alfred Rufer, Drazen Dujic, Francisco Canales, and Yales Romulo De Novaes. Isolated dc/dc structure based on modular multilevel converter. *IEEE Transactions on Power Electronics*, 30(1):89–98, 2015.

[29] B. Li, Z. Xu, and D. Xu. Control schemes of the front-to-front (ftf) power electronic topologies for future HVDC interconnections. In *Proc.*

Asia-Pacific (ITEC Asia-Pacific) 2017 IEEE Transportation Electrification Conf. and Expo, pages 1–6, August 2017.

[30] I. A. Gowaid, G. P. Adam, S. Ahmed, D. Holliday, and B. W. Williams. Analysis and design of a modular multilevel converter with trapezoidal modulation for medium and high voltage DC-dc transformers. *IEEE Transactions on Power Electronics*, 30(10):5439–5457, October 2015.

[31] I. A. Gowaid, G. P. Adam, A. M. Massoud, S. Ahmed, D. Holliday, and B. W. Williams. Quasi two-level operation of modular multilevel converter for use in a high-power DC transformer with DC fault isolation capability. *IEEE Transactions on Power Electronics*, 30(1):108–123, January 2015.

[32] T. Lüth, M. M. C. Merlin, T. C. Green, F. Hassan, and C. D. Barker. High-frequency operation of a DC/AC/DC system for HVDC applications. *IEEE Transactions on Power Electronics*, 29(8):4107–4115, August 2014.

[33] I. A. Gowaid, G. P. Adam, A. M. Massoud, S. Ahmed, and B. W. Williams. Hybrid and modular multilevel converter designs for isolated HVDC –DC converters. *IEEE Journal of Emerging and Selected Topics in Power Electronics*, 6(1):188–202, March 2018.

[34] Y. Hu, G. Chen, Y. Liu, L. Jiang, P. Li, S. J. Finney, W. Cao, and H. Chen. Fault-tolerant converter with a modular structure for HVDC power transmitting applications. *IEEE Transactions on Industry Applications*, 53(3):2245–2256, May 2017.

[35] X. Zhang and T. C. Green. The new family of high step ratio modular multilevel DC-dc converters. In *Proc. IEEE Applied Power Electronics Conf. and Exposition (APEC)*, pages 1743–1750, March 2015.

[36] D. Jovcic. Bidirectional, high-power DC transformer. *IEEE Transactions on Power Delivery*, 24(4):2276–2283, October 2009.

[37] D. Jovcic and L. Zhang. Lcl DC/dc converter for DC grids. *IEEE Transactions on Power Delivery*, 28(4):2071–2079, October 2013.

[38] J. Yang, Z. He, H. Pang, and G. Tang. The hybrid-cascaded DC –DC converters suitable for hvdc applications. *IEEE Transactions on Power Electronics*, 30(10):5358–5363, October 2015.

[39] X. Zhang and T. C. Green. The modular multilevel converter for high step-up ratio DC –DC conversion. *IEEE Transactions on Industrial Electronics*, 62(8):4925–4936, August 2015.

[40] A. Schön and M. M. Bakran. A new HVDC-DC converter with inherent fault clearing capability. In *Proc. 15th European Conf. Power Electronics and Applications (EPE)*, pages 1–10, September 2013.

[41] W. Lin. DC –DC autotransformer with bidirectional DC fault isolating capability. *IEEE Transactions on Power Electronics*, 31(8):5400–5410, August 2016.

[42] G. J. Kish. On the emerging class of non-isolated modular multilevel DC-dc converters for DC and hybrid AC-DC systems. *IEEE Transactions on Smart Grid*, page 1, 2017.

[43] W. Lin, J. Wen, and S. Cheng. Multiport DC –DC autotransformer for interconnecting multiple high-voltage DC systems at low cost. *IEEE Transactions on Power Electronics*, 30(12):6648–6660, December 2015.

[44] Dirk Van Hertem, Oriol Gomis-Bellmunt, and Jun Liang. *HVDC Technology and Technology for Offshore Grids*, pages 528–. Wiley-IEEE Press, 2016.

[45] Regional investment plan 2015 north sea region. Technical report, ENTSO-E, 2015.

[46] Québec - new england the first large scale multiterminal hvdc transmission in the world to be upgraded. https://new.abb.com/systems/hvdc/references/quebec-new-england.

[47] Franco Mazzoldi, Jean Pierre Taisne, Christopher J.B. Martin, and Brian A. Rowe. Adaptation of the control equipment to permit 3-terminal operation of the hvdc link between sardinia, corsica and mainland italy. *IEEE Transactions on Power Delivery*, v:1269–1274, 1992.

[48] J. Duncan Glover and Mulukutla S Sarma. *Power system analysis and design.* Thomson Learning. Brooks/Cole, Pacific Grove, 3rd ed. edition, 2001.

[49] Jun Liang Jorge Gonçalves, Daniel J. Rogers. Extension of power transmission capacity in mmc-based hvdc systems through dynamic temperature-dependent current. In *Conference: Power Electronics and Applications (EPE'15 ECCE-Europe)*. Cardiff University, 2015.

[50] J. Schachner. Power connections for offshore wind farms. Master's thesis, Delft University of Technology, January 2004.

[51] Renewables-technology overview compact hvdc solutionsn. https://www.siemens.com/global/en/home/products/energy/high-voltage/grid-access-solutions.html.

[52] Sara Knight. Analysis: Siemens' radical substation plan. https://www.windpoweroffshore.com/article/1338456/analysis-siemens-radical-substation-plan, 2015.

[53] Siemens. Siemens new dc grid access solution. http://m.energy.siemens.com/hq/pool/hq/power-transmission/grid-access-solutions/dc-solutions/DC-Flyer.pdf.

[54] Onno Groß. Seimens: Offshore wind power, mighty efficient. https://www.siemens.com/customer-magazine/en/home/energy/power-transmission-and-distribution/mighty-efficient-offshore-grid-access.html, 2015.

[55] Dr Jan Declercq and Raymond Van Schevensteen. Challenges for reliable offshore transformers. maximising the value of wind energy. Technical report, Pauwels International NV, Belgium, 2008.

[56] Abb develops complete system solution for 1,100 kv hvdc power transmission. http://www.abb.com/cawp/seitp202/d83ce03a99b85dd7c1257d400041aab5.aspx.

[57] Abb achieves breakthrough with world's most powerful hvdc transformer. https://new.abb.com/news/detail/2718/ABB-achieves-breakthrough-with-worlds-most-powerful-hvdc-transformer.

[58] Til Kristian Vrana and Raymundo E Torres Olguin. Technology perspectives of the north sea offshore and storage network (nson). Technical report, SINTEF, 2015.

[59] L. Shi, C. Shan, X. Wu, and N. Zhao. Comparison of solid-state frequency converter and rotary frequency converter in 400hz power system. In *2011 International Conference on Electrical Machines and Systems*, pages 1–5, Aug 2011.

[60] Y. Takemoto, G. Fujita, K. Hasegawa, K. Koyanagi, T. Funabashi, and R. Yokoyama. Experimental study on rotary frequency converter. In *Proceedings of the 13th International Conference on, Intelligent Systems Application to Power Systems*, pages 6 pp.–, Nov 2005.

[61] Jonathan Ruddy, Ronan Meere, and Terence Odonnell. A comparison of vsc-hvdc with low frequency ac for offshore wind farm design and interconnection. *Energy Procedia*, 80(C):185–192, 2015.

[62] H. Wiechmann and K. Tischler. Mining technologies comparison of alternative converters with regard to their application for gearless drives for grinding mills. Technical report, September 2007.

[63] Siemens dcgi switch gear space-saving, flexible, reliable 320kv dc compact switchgear. https://www.energy.siemens.com/hq/pool/hq/power-transmission/HVDC/innovations/DCCS-Brochure.pdf.

[64] Carlos E Ugalde-Loo*1 Paul Coventry*2 Gen Li*1, Jun Liang*1. Impacts of dc circuit breakers on ac/dc system stability subject to dc faults. In *International High Voltage Direct Current Conference*. *1 Institute of Energy and Environment, Cardiff University, Cardiff, UK. *2 National Grid, Warwick Technology Park, Warwick, UK, 2016.

[65] Abb's hybrid hvdc circuit breaker. https://new.abb.com/grid/events/cigre2014/hvdc-breaker.

[66] Rizk FAM. A systematical approach to high voltage insulator selection for polluted environment. Amman, Jordan, May 1997.

[67] Narain G Hingorani and Laszlo Gyugyi. *Understanding FACTS : concepts and technology of flexible AC transmission systems*. IEEE Press, New York (N.Y.), 2000.

[68] E. Camm D. Mueller J. Schoene T. Siebert T. Smith M. Starke R. Walling M. Bradt, B. Badrzadeh. Harmonics and resonance issues in wind power plants. *IEEE PES Wind Plant Collector System Design Working Group*, 2012.

[69] T.E. McDermott. Distributed wind evaluation methodology. *AWEA WindPower*, 2009.

[70] H. Fujita and H. Akagi. A practical approach to harmonic compensation in power systems-series connection of passive and active filters. *IEEE Transactions on Industry Applications*, 27(6):1020–1025, Nov 1991.

[71] Joakim Gerggren. Study of auxiliary power systems for offshore wind turbines. Master's thesis, UPPSALA Universitet, June 2013.

[72] Fabio Terezinho. Scada systems automate electrical distribution. InduSoft, 2015.

[73] A. Shahzad, S. Musa, A. Aborujilah, and M. Irfan. The scada review: System components, architecture, protocols and future security trends. *American Journal of Applied Sciences*, 11(8):1418–1425, 2014.

[74] Rosario Miceli. Energy management and smart grids. *Energies*, 6(4):2262–2290, 2013.

[75] M. L. Chan and W. H. Crouch. An integrated load management, distribution automation and distribution scada system for old dominion electric cooperative. *IEEE Transactions on Power Delivery*, 5(1):384–390, Jan 1990.

[76] Steps to establish a real-time transmission monitoring system for transmission owners and operators within the eastern and western interconnections. Technical report, United States Department of Energy & Federal Energy Regulatory Commission, 2006.

[77] Morten Holmager, editor. *Offshore Book An introduction to the offshore industry*. Offshore center Denmark.

[78] Paraic Higgins and Aoife Foley. The evolution of offshore wind power in the united kingdom. *Renewable and Sustainable Energy Reviews*, 37:599 – 612, 2014.

[79] Katharina Garius. Eew has produced the world's heaviest monopile. http://www.offshorewindindustry.com/news/eew-produced-worlds-heaviest-monopile, March 2016.

[80] Carbon Trust. Floating offshore wind: Market and technology review. Technical report, June 2015.

[81] Shane Butler. *Prognostic Algorithms for Condition Monitoring and Remaining Useful Life Estimation*. PhD thesis, National University of Ireland Maynooth, 2012.

[82] P. Bauer M.Pavlovsky. Cable selection and shunt compensation for offshore windparks. Delf University of Technology, 2003.

[83] M C Merlin T.C. Green X. Xiang, M. Cost analysis and comparison of hvac, lfac and hvdc for offshore wind power connection. In *The 12th IET International Conference on AC and DC Power Transmission (ACDC 2016)*, 2016.

[84] U.S. Satpute and D.R. Joshi. Optimum frequency-based design of offshore wind power plant (owpp). volume 2017-, pages 1–6. IEEE Computer Society, March 2018.

[85] *Journal of Environmental Science, Computer Science and Engineering and Technogy*, 80(E-ISSN: 2278-179X):185–192, September 2013.

[86] M. Zubiaga, G. Abad, J.A. Barrena, S. Aurtenetxea, and A. CÃ¡rcar. Evaluation and selection of ac transmission lay-outs for large offshore wind farms. In *2009 13th European Conference on Power Electronics and Applications, EPE '09*, 2009.

[87] O. Bolado M. Bollen M. Bradt C. Brooks W. Dilling M. Edds W. J. Hejdak D. Houseman S. Klein F. Li J. Li P. Maibach T. Nicolai J. Patiño S. V. Pasupulati N. Samaan S. Saylors T. Siebert T. Smith

M. Starke R. Walling E.H. Camm, M. R. Behnke. Wind power plant substation and collector system redundancy, reliability, and economics. *IEEE PES Wind Plant Collector System Design Working Group*, 2009.

[88] Stefan Lundberg. *Wind Farm Configuration and Energy Efficiency Studies - Series DC versus AC Layouts.* PhD thesis, Department of Energy and Environment Chalmers University of Technology Goteborg, Sweden, 2006.

[89] H. Chen, M. H. Johnson, and D. C. Aliprantis. Low-frequency ac transmission for offshore wind power. *IEEE Transactions on Power Delivery*, 28(4):2236–2244, Oct 2013.

[90] A. Prasai, D. Jung-Sik Yim, A. Divan, A. Bendre, and A. Seung-Ki Sul. A new architecture for offshore wind farms. *Power Electronics, IEEE Transactions on*, 23(3):1198–1204, May 2008.

[91] S. Lumbreras and A. Ramos. Optimal design of the electrical layout of an offshore wind farm applying decomposition strategies. *IEEE Transactions on Power Systems*, 28(2), August 2012.

[92] A. Madariaga, I. Martínez de Alegría, J.L. Martín, P. Eguía, and S. Ceballos. Current facts about offshore wind farms. *Renewable and Sustainable Energy Reviews*, 16(5):3105 – 3116, 2012.

[93] A. Madariaga, J.L. Martín, I. Zamora, I. Martínez de Alegría, and S. Ceballos. Technological trends in electric topologies for offshore wind power plants. *Renewable and Sustainable Energy Reviews*, 24:32 – 44, 2013.

[94] M. Abbasi and J. Lam. A step-up transformerless, zv –ZCS high-gain DC/dc converter with output voltage regulation using modular step-up resonant cells for DC grid in wind systems. *IEEE Journal of Emerging and Selected Topics in Power Electronics*, 5(3):1102–1121, September 2017.

[95] T. Ruddy R. A. Walling. Economic optimization of offshore windfarm substations and collection systems. *GE Energy*, March 2005.

[96] Massimo Gracchi, Luigi Meroni, and Piergiorgio Betteto. A new way for access and maintenance of offshore wind farms: The use of cableway

to reduce cost and improve accessibility. *Wind Engineering*, 37(3):281–303, June 2013.

[97] M. Dicorato, G. Forte, M. Pisani, and M. Trovato. Guidelines for assessment of investment cost for offshore wind generation. *Renewable Energy*, 36(8):2043–2051, 2011.

[98] DTI Department of Trade and Industry contractor ODE Limited. Study of the costs of offshore wind generation. Technical report, 2007.

[99] S. Lundberg. Performance comparison of wind park configuration. technical report. Technical report, Chambers University of Technology, Goteborg, Sweden, 2003.

[100] Mcgowan JG Elkinton CN, Manwell JF. Offshore wind farm layout optimization (owflo) project: an introduction. In *2005 offshore wind conference and exhibition, Copenhagen*, October 2005.

[101] Nielsen P. Offshore wind energy projects feasibility study guidelines. seawind altener project. Technical report, June 2003.

[102] Terna. Conventional technical solution for the connection to main power system - average grid component costs report (in italian). http://www.terna.it. Technical report, 2008.

[103] JLazaros P. Lazaridis. Economic comparison of hvac and hvdc solutions for large offshore wind farms under special consideration of reliability. Master's thesis, Royal Institute of Technology, 2005.

[104] T. Lagier, P. Ladoux, and P. Dworakowski. Potential of silicon carbide mosfets in the DC/dc converters for future HVDC offshore wind farms. *High Voltage*, 2(4):233–243, 2017.

[105] Hajir Pourbabak and Ahad Kazemi. A new technique for islanding detection using voltage phase angle of inverter-based dgs. *International Journal of Electrical Power & Energy Systems*, 57:198 – 205, 2014.

[106] S. Kar, G. Hug, J. Mohammadi, and J. M. F. Moura. Distributed state estimation and energy management in smart grids: A consensus+ innovations approach. *IEEE Journal of Selected Topics in Signal Processing*, 8(6):1022–1038, Dec 2014.

[107] G. Gerdes, A. Tiedemann, and S. Zeelenberg. Case study: European offshore wind farms - a survey for the analysis of the experiences and lessons learnt by developers of offshore wind farms. Technical report, Deutsche WindGuard and German Energy Agency (DENA) and University of Groningen, 01/08 2008.

[108] Study of the costs of offshore wind generation. Technical report, Offshore Design Engineering (ODE) Limited, 2007.

[109] C A Morgan, H M Snodin, and N C Scott. Offshore wind economies of scale, engineering resource and load factors. Technical report, Dept of Trade and Industry / Carbon Trust, 2003.

[110] Wireless solar communications technology reduces cost and is easier to maintain, 2016. SunEnergy1 & Duke Energy Renewables.

[111] J. Ribrant and L. Bertling. Survey of failures in wind power systems with focus on swedish wind power plants during 1997-2005. pages 1–8. IEEE, June 2007.

[112] A. Sannino, H. Breder, and E.K. Nielsen. Reliability of collection grids for large offshore wind parks. pages 1–6. IEEE, June 2006.

[113] J. Yang, J. O'Reilly, and J. E. Fletcher. Redundancy analysis of offshore wind farm collection and transmission systems. In *2009 International Conference on Sustainable Power Generation and Supply*, pages 1–7, April 2009.

[114] M. Stojkov, S. Nikolovski, and V. Mikulicic. Estimation of electrical energy not supplied in reliability analysis of distribution networks. In *Proceedings of the 12th IEEE Mediterranean Electrotechnical Conference (IEEE Cat. No.04CH37521)*, volume 3, pages 967–970 Vol.3, May 2004.

[115] A. G. Bruce. Reliability analysis of electric utility scada systems. In *Proceedings of the 20th International Conference on Power Industry Computer Applications*, pages 200–205, May 1997.

[116] J. Formea and J. Gadbury. Improve power reliability through small-scale scada systems. In *2016 IEEE Rural Electric Power Conference (REPC)*, pages 21–26, May 2016.

[117] E. Keith Stanek Kelvin T. Erickson, Ann Miller and Shari Dunn-Norman. Survey of scada system technology and reliability in the offshore oil and gas industry. Technical report, University of Missouri-Rolla, 2000.

[118] Lingling Huang and Yang Fu. Reliability evaluation of the offshore wind farm. pages 1–5. IEEE Publishing, March 2010.

[119] Dusko P. Nedic*2 Muhammad Ali*1 and J. V. Milanovic*3. Robust methodology for cost-effective design of large offshore wind farms. *1-TNEI Services Ltd., Manchester, UK. *2-Siemens PTI, Manchester, UK. *3-School of Electrical and Electronic Engineering, The University of Manchester, UK.

[120] CIGRE Task Force 33.04.01. Polluted insulators : a review of current knowledge., June 2000.

[121] CIGRE Working Group 33-04. The measurement of site pollution severity and its application to insulator dimensioning for AC systems. *Electra*, No. 64:101–116, 1979.

[122] NGK. *Technical Guide, Cat. No. 91 R, First Revision.* 1989.

[123] G. Kaiser. The mouse buzzard as a cause of breakdowns on 110 kV single pole high-tension lines. *Elecktrotechnische Zietschrift*, 1970.

[124] H. J. West, J. E. Brown, and A. L. Kinyon. Simulation of EHV transmission line flashovers initiated by, bird excretion. *IEEE Transactions on Power Apparatus and Systems*, (4):1627–1630, 1971.

[125] J. T. Burnham. Bird streamer flashovers on FPL transmission lines. *IEEE Transactions on Power Delivery*, 10(2):970–977, 1995.

[126] Lightning and Insulator Subcommittee IEEE Working Group on Insulator Contamination. Application of insulators in a contaminated environment. *IEEE Trans. on Power Apparatus and Systems*, Vol. PAS-98, No. 5:pp. 1676–1695, October 1979.

[127] J. S. T. Looms. *Insulators for high voltages.* Number 7. IET, 1988.

[128] A. K. Gertsik, A. V. Korsuntser, and N. K. Nikol'Skii. The effect of fouling on insulators for HVDC overhead lines. *Direct current*, 3:219–226, 1957.

[129] A. Annestrand and A. Schei. A test procedure for artificial pollution tests on direct voltage. *Direct Current*, 12(1):1–8, 1967.

[130] James F. Hall and T. Paul. Wind tunnel studies of the insulator contamination process. *IEEE Transactions on Electrical Insulation*, (3):180–188, 1981.

[131] H. M. Schneider and C. W. Nicholls. Contamination flashover performance of insulators for UHV. *IEEE Transactions on Power Apparatus and Systems*, (4):1411–1420, 1978.

[132] W. Lampe, T. K. E. Hoglund, C. L. Nellis, P. E. Renner, and R. D. Stearns. Long-term tests of HVDC insulators under natural pollution conditions at the Big Eddy Test Center. *IEEE Transactions on Power Delivery*, 4(1):248–259, 1989.

[133] A. C. Baker, L. E. Zaffanella, L. D. Anzivino, H. M. Schneider, and J. H. Moran. Contamination performance of HVDC station post insulators. *IEEE transactions on power delivery*, 3(4):1968–1975, 1988.

[134] D Wu, R Hartings, U Aström, B Almgren, and S Nord. The performance of station post insulators for UHVDC applications. In *10th International Symposium on High Voltage Engineering (ISH)*, volume 3, pages 41–44, Montreal, Canada, August 1997.

[135] CIGRE Working Group C4.303. Outdoor insulation in polluted conditions:Guidelines for selection and dimensioning - PART 2: THE DC CASE, December 2012.

[136] Ouahid Dahmani, Salvy Bourguet, Mohamed Machmoum, Patrick Guerin, and Pauline Rhein. Reliability analysis of the collection system of an offshore wind farm. pages 1–6. IEEE, March 2014.

[137] Richard E Stephens. A method for economic evaluation of distribution transformers. *Report of the Eei Task Force on Distribution Transformer Evaluation. Washington, D.C.*, 1981.

[138] Ouahid Dahmani, Salvy Bourguet, Mohamed Machmoum, Patrick Guerin, Pauline Rhein, and Lionel Josse. Optimization and reliability evaluation of an offshore wind farm architecture. *Sustainable Energy, IEEE Transactions on*, 8(2):542–550, April 2017.

[139] Sara Lumbreras, Andres Ramos, and Santiago Cerisola. A progressive contingency incorporation approach for stochastic optimization problems. *Power Systems, IEEE Transactions on*, 28(2):1452–1460, May 2013.

[140] S. Lumbreras and A. Ramos. Offshore wind farm electrical design: a review. *Wind Energy*, 16(3):459–473, April 2013.

[141] Hakan Ergun, Dirk Van Hertem, and Ronnie Belmans. Transmission system topology optimization for large-scale offshore wind integration. volume 3. IEEE, 2013.

[142] Martin Vastermark. Grid code compliance - wind farm connection. Technical report, Uppsala Universitet, March 2013.

[143] Predrag Djapic and Goran Strbac. Cost benefit methodology for optimal design of offshore transmission systems. Technical report, BERR Department for Business Enterprise and Regulatory Reform, July 2008.

[144] M. Banzo and A. Ramos. Stochastic optimization model for electric power system planning of offshore wind farms. *Power Systems, IEEE Transactions on*, 26(3):1338–1348, August 2011.

[145] Roger J-B Wets. *Algorithms and Modelling in Mathematical Programming*, pages 91–113. S. Wallace, Springer-Verlag, Berlin, 1989.

[146] Dirk Van Hertem Hakan Ergun and Frederik Geth. Powermodelsacdc repository. https://github.com/hakanergun/PowerModelsACDC.jl, 2018.

[147] Dirk Van Hertem Hakan Ergun, Jay Dave and Frederik Geth. Optimal power flow for ac/dc grids: Formulation, convex relaxation, linear approximation and implementation. Submitted to IEEE Transactions on Power Systems, 2018.

[148] Yogesh Kumar, Jordan Ringenberg, Soma Shekara Depuru, Vijay K. Devabhaktuni, Jin Woo Lee, Efstratios Nikolaidis, Brett Andersen, and Abdollah Afjeh. Wind energy: Trends and enabling technologies. *Renewable and Sustainable Energy Reviews*, 53:209 – 224, 2016.

[149] Repower 6.2m126 offshore. https://en.wind-turbine-models.com/turbines/291-repower-6.2m126-offshore.

[150] N. Luo. Analysis of offshore support structure dynamics and vibration control of floating wind turbines. In *Proceedings of the 31st Chinese Control Conference*, pages 6692–6697, July 2012.